

# Chirality Production with Mass Effects–Schwinger Pair Production and the Axial Ward Identity

Patrick Copinger

*Theory Center, Institute of Particle and Nuclear Studies,  
High Energy Accelerator Research Organization (KEK)  
1-1 Oho, Tsukuba, Ibaraki 305-0801, Japan*

*Department of Physics and Center for Field Theory and Particle Physics,  
Fudan University, 220 Handan Rd., Shanghai 200433, China  
copinger@post.kek.jp*

Shi Pu

*Department of Modern Physics and Interdisciplinary Center for Theoretical Study,  
University of Science and Technology of China, Hefei, Anhui 230026, China  
shipu@ustc.edu.cn*

The anomalous generation of chirality with mass effects via the axial Ward identity and its dependence on the Schwinger mechanism is reviewed, utilizing parity violating homogeneous electromagnetic background fields. The role vacuum asymptotic states play on the interpretation of expectation values is examined. It is discussed that observables calculated with an in-out scattering matrix element predict a scenario under Euclidean equilibrium. A notable ramification of which is a vanishing of the chiral anomaly. In contrast, it is discussed observables calculated under an in-in, or real-time, formalism predict a scenario out-of equilibrium, and capture effects of mean produced particle anti-particle pairs due to the Schwinger mechanism. The out-of equilibrium chiral anomaly is supplemented with exponential quadratic mass suppression as anticipated for the Schwinger mechanism. Similar behavior in and out-of equilibrium is reviewed for applications including the chiral magnetic effect and chiral condensate.

*Keywords:* Chiral Anomaly; Schwinger Mechanism; Nonequilibrium Quantum Field Theory.

PACS numbers: 05.70.Ln, 11.30.Rd, 12.20.-m

## 1. Introduction

An anomaly manifests itself for systems with a symmetry that, while at a classical level is realized, is actually broken at the quantum level. For relativistic fermionic systems the chiral symmetry<sup>1</sup> gives rise to such an anomaly, and the breaking of the chiral symmetry is of paramount importance for several phenomena, notably including imparting the bulk of the visible mass to the universe.<sup>2,3</sup> The direct observation of the chiral anomaly, however, remains, and an essential application of the anomaly that may facilitate its observation is the chiral magnetic effect (CME).

The CME is an electromagnetic current in the presence of and along the direction of a magnetic field due to a net chirality.<sup>4</sup> Relativistic fermionic dispersion relations

are realizable in 2D and 3D condensed matter systems for Weyl and Dirac semimetals.<sup>5–8</sup> And, in a Dirac semimetal the CME was thought to be observed.<sup>9</sup> Even so, it is still challenging to observe the CME in relativistic heavy-ion collisions due to huge background contributions, despite a strong magnetic field thought present—in fact, a field as large as  $eB \sim m_\pi^2$  may be possible<sup>10</sup>—in off-central collisions.

The presence of the other ingredient of the CME, namely a net chirality, in colliders comes with greater uncertainty. And it is an uncertainty one may mitigate with an improved understanding of how chirality is generated. We address the following three issues in this review:

- (1) Chirality imbalance frequently is inserted by hand, usually by means of a chiral chemical potential. However, while a useful theoretical tool, there are instances where such insertions are inadequate. One such case lies with systems well out-of-equilibrium.
- (2) The behavior of the chiral anomaly and magnetic effect in and out-of-equilibrium requires elucidation. The out-of-equilibrium case is prominent in heavy-ion collisions. There a glasma,<sup>11,12</sup> or dense gluonic state, is thought to give rise to parity-violating flux tubes and the accompanying chiral anomaly and CME.<sup>13</sup>
- (3) Finally, what are the effects of a finite mass on the chiral anomaly and CME? While in high energy applications it is common to dismiss the mass—e.g., a pseudoscalar term, we will go on to argue that this dismissal is not subtle.

The answer to the above questions can be addressed through the Schwinger mechanism. In a background electric field the quantum field theoretic (QFT) vacuum is thought to be unstable against the creation of particle anti-particles pairs through tunneling in what is known as the Schwinger mechanism. The QCD electric field analog is provided by chromo-electric flux tubes, whose breaking is facilitated through the Schwinger mechanism leading to hadronization.<sup>14</sup> How might one furnish a net chirality from the Schwinger mechanism? This is thought possible with a parallel strong magnetic field, setting up a parity-violating background. Then predicted pairs of particles have their spins aligned with the magnetic field generating a net chirality.<sup>13,15</sup> This phenomenon has also been studied numerically.<sup>16–18</sup>

The axial Ward identity provides an appropriate means of accessing the chirality non-conservation for massive fermionic systems,<sup>19,20</sup> and is composed of both a contribution due to quantum effects as well as a massive pseudoscalar term. Taking expectation values of the axial Ward identity, however, using standard treatments lead to puzzling results in contrast to the picture of chirality generation via the Schwinger mechanism; notably a conservation of chirality can be found.

A clear identification of vacuum states and their expectation values provides a resolution.<sup>21</sup> Usage of either in-out or in-in vacuum states predict decidedly different physical scenarios. The expectation values of in-out vacuum states, used in standard approaches, predict a scenario of Euclidean equilibrium. However, the Schwinger mechanism—and hence chiral driven phenomena—is inherently out-of-equilibrium, and the real-time process of pair production is not captured with an in-out formal-

ism. It is, however, captured utilizing an in-in, (or Schwinger-Keldysh), formalism. There a chirality non-conservation is predicted out-of equilibrium in accordance with the Schwinger mechanism, as evidenced by an exponential quadratic mass suppression. This has implications for theories built on an anomaly, e.g. for baryogenesis driven by a parity-violating inflaton,<sup>22</sup> as well as experimental ramifications. In addition to the chiral anomaly by the axial Ward identity, we also examine the CME as well as the chiral condensate.

Even though a system possesses no global net chirality, this does not mean that it might not be present locally. This is thought to be the case in heavy-ion collisions.<sup>23,24</sup> One way one might characterize a local non-conservation of chirality is through an examination of chiral density fluctuations, or a chiral susceptibility. Similar in and out-of equilibrium behavior, with characteristic Schwinger mechanism signatures, is noted for such correlated observables.

The enhancement of the chiral condensate, or rather a dynamically driven mass, by a background magnetic field is known as magnetic catalysis.<sup>25–27</sup> However, how is the chiral condensate augmented by an electric field and the Schwinger pair production process in and out-of equilibrium? We address this here too. It is found the electric field serves to diminish the condensate, and for strong enough fields may even negate the condensate all together.

The structure of this review along with notations are given as follows: To supplement the cursory look at the generation of chirality via the Schwinger mechanism just offered, we give some background to the chiral anomaly and magnetic effects in Sec. 2 and to the Schwinger mechanism in Sec. 3. Then a heuristic picture of chirality generation from the Schwinger mechanism is presented in Sec. 4. Next we proceed with the identification of vacuum states and their importance in the interpretation of expectation values in Sec. 5. Next, the application of vacuum states to the generation of chirality through the axial Ward identity is discussed in Sec. 6. Then extensions to other chiral anomaly related phenomena including the CME in Sec. 7, and the chiral condensate in Sec. 8 are discussed. Last, a conclusion to the review is presented in Sec. 9.

The following notations are used in this review: We use a mostly minus metric,  $g = \text{diag}(+, -, -, -)$ , and whenever appropriate contracted Lorentz indices are implicit, i.e.,  $A_\mu B^\mu =: AB$ . Our covariant derivative reads  $D_\mu = \partial_\mu + ieA_\mu$ . And we also use units such that  $c = \hbar = 1$ . For gamma matrices a Weyl representation is used:

$$\gamma^0 = \begin{pmatrix} I_2 & \\ & I_2 \end{pmatrix}, \quad \gamma^i = \begin{pmatrix} & \sigma^i \\ -\sigma^i & \end{pmatrix}, \quad \gamma_5 = \begin{pmatrix} -I_2 & \\ & I_2 \end{pmatrix}, \quad (1)$$

with  $\sigma^i$  being the Pauli matrices. The spin tensor reads  $\sigma_{\mu\nu} = \frac{i}{2}[\gamma_\mu, \gamma_\nu]$ . Last, point split observables are evaluated with an averaged propagator as in  $S(x, x) = \frac{1}{2} \lim_{\epsilon \rightarrow 0} [S(x, x + \epsilon) + S(x + \epsilon, x)]$ ; elsewhere we take for Heaviside functions  $\lim_{x \rightarrow 0} \theta(x) = [\theta(0^+) + \theta(0^-)]/2 = 1/2$ .

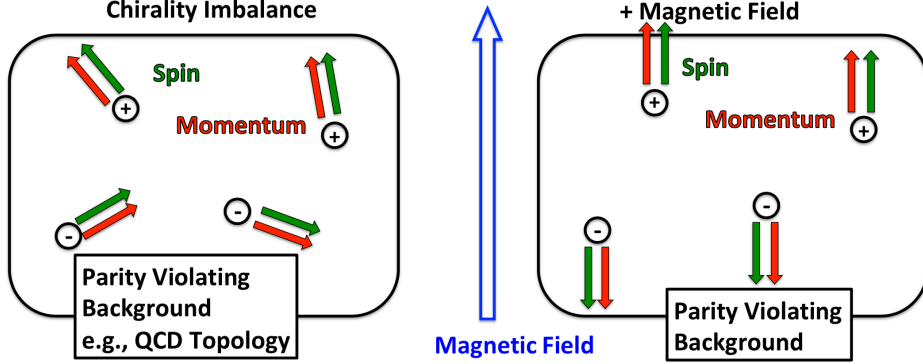


Fig. 1. Diagram of the CME process. (Left) A non-conservation of chirality is dictated due to the chiral anomaly in a topologically non-trivial QCD background. Green and red arrows represent spin and momentum vectors respectively. Plus and minus circles represent particles and anti-particles respectively. A net chirality difference of  $\Delta N_5 = 4$  is shown. (Right) A strong magnetic field is then added, projecting the particles' spins and setting up an electromagnetic current in what is known as the CME.

## 2. Chiral Anomaly and Magnetic Effect

Anomalous phenomena are ubiquitous throughout physics and can be responsible for constraints on conserved currents, symmetries, and spectrums of a theory. A clear manifestation of the anomaly in experiment is provided by the decay of a neutral pion into two photons: While classically forbidden, it was found at a quantum level<sup>19,28</sup> the process be achievable.

One may characterize the anomaly of QCD with a topological  $\theta$  term.<sup>29</sup> In QCD the Lagrangian can be supplemented with  $\frac{\theta}{32\pi}\epsilon_{\mu\nu\alpha\beta}G^{\mu\nu a}G^{\alpha\beta a}$  for gluon field strength  $G$  in  $SU(3)$ , and is both  $\mathcal{P}$  (parity) and  $\mathcal{CP}$  (charge-parity) violating. Unfortunately, there is no strong evidence to prove such a term really exists in experiments—neutron dipole moments are restricted to  $|d_n| < 2.9 \times 10^{-26} e \text{ cm}$ ,<sup>30</sup> the theoretical underpinning of this problem is called the “strong  $\mathcal{CP}$  problem.” However, there may be environments where topology may be present, if only locally. This is thought to be the case in quark-gluon plasmas, giving rise to a axion-like topological term with space-time dependence,<sup>31</sup> i.e.,  $\theta \rightarrow \theta(x)$ . A consequence of which is a manifestation of an electromagnetic current, the CME.

Due to a non-trivial topology, a chirality non-conservation is dictated through the chiral anomaly. And in the context of a heavy-ion collision—for example—with a strong transverse to reaction plane magnetic field coupled with a net chirality, the CME is thought to arise. Let us elaborate on the essential physics. See Fig. 1 for the CME process.

The left diagram depicts the chiral anomaly, where for a  $\mathcal{P}$  violating background, such as for a topologically non-trivial background in a quark-gluon plasma, a net chirality is furnished. We have made the assumption here of massless particles, which entails that particle chirality and helicity be similar, and anti-particles have chirality

opposite to their helicity. This amounts to a net chirality difference given as the total number of particles plus antiparticles with right-handed helicity minus the total with left-handed helicity.<sup>4</sup> Right (left)-handed helicity is given by parallel (anti-parallel) spin and momentum vectors, which we can denote figuratively as  $h_{R(L)}$  and  $\bar{h}_{R(L)}$  for particles and antiparticles respectively. In other words  $\Delta N_5 = \sum h_R + \bar{h}_R - h_L - \bar{h}_L$ . Then, in the right diagram in Fig. 1, a strong magnetic field is added. The lowest Landau level is occupied, projecting the particles' spins to the direction of the magnetic field, giving rise to an electromagnetic current, the CME. The process may also be understood as arising from the Dirac sea coupled with the chiral anomaly,<sup>31</sup> however we reserve such discussions till Sec. 4.

Enormous experimental effort has been carried out for the CME both in condensed matter and collider environments. Notably, the CME was thought to be observed in a semimetal.<sup>9</sup> However, in heavy-ion collision experiments, such as at the the large hadron collider (LHC) at CERN and the relativistic heavy ion collider (RHIC) at the Brookhaven National Laboratory, the CME has yet to be confirmed.

Relativistic fermionic dispersion relations, as well as the chiral anomaly and CME, were thought producible in a number of condensed matter environments including graphene and Weyl and Dirac semimetals, and spin-orbit coupled atomic gases.<sup>32</sup> Let us describe and confine our attention to the former. In contrast to a semi-conductor, the semimetal's/ graphene's valence and conduction bands possess a small overlap permitting novel electronic and transport properties. Notably, a chirality can be governed at the Weyl nodes, which serve as topological charges formed from a Berry's curvature in crystal quasi-momentum space.<sup>33,34</sup> A relativistic massless Weyl-like fermionic quasi-particle excitation and spectrum were discovered in a 2+1 dimensional graphene<sup>35</sup> and a 3+1 dimensional semimetal.<sup>5,6,36,37</sup> Accordingly, the anomaly was thought to be found in a Weyl semimetal,<sup>38</sup> as well as, through a negative magnetoresistance<sup>39</sup> signature, the CME was thought to be found in a semimetal.<sup>9</sup>

In the strong magnetic fields present in off-central heavy-ion collisions, the CME is thought to be observable due to a local parity violation. Even though topological fluctuations are not directly observable in collisions, charge asymmetries of event-by-event correlations may be observable.<sup>40</sup> Such measurements have been performed by groups STAR at the RHIC<sup>41</sup> and ALICE at the LHC.<sup>42</sup> However, while results are consistent with local parity violation and the CME, background interference cannot be mitigated, and thus verification of the CME in colliders cannot be accomplished quite yet.<sup>40</sup>

In addition, the magnetic fields can also induce a chiral current, which is named Chiral Separation Effect (CSE).<sup>23,43,44</sup> The collective modes of CME combined with CSE are called Chiral Magnetic Waves, which are also an important topic in relativistic heavy ion collisions.<sup>45,46</sup> There are also many higher order nonlinear quantum phenomena related to electromagnetic fields, e.g., the chiral electric or Hall separation effects<sup>47–50</sup> and other effects coupled to the gradient of temperature or chemical potentials.<sup>51–59</sup>

There are two ways to investigate the CME and other chiral transport phenomena. The microscopic description of the CME is called the chiral kinetic theory (CKT), which is the quantum kinetic theory for the massless fermions. CKT can be derived from the path integrals,<sup>60–63</sup> effective theories,<sup>64–68</sup> Wigner function approaches<sup>69–77</sup> and world-line formalism.<sup>78,79</sup> Based on CKT, several numerical simulations for relativistic heavy ion collisions appear.<sup>80–87</sup> The quantum kinetic theory for the massive fermions<sup>88–94</sup> and collisional terms<sup>95,96</sup> are also widely discussed recently.

Another way to study CME is through the macroscopic effective theories based on the hydrodynamic equations coupled to the Maxwell's equations. One framework is named the relativistic magnetohydrodynamics,<sup>97–103</sup> which has been widely used in astrophysics. The recent studies have been extended to the system in the presence of CME and chiral anomaly.<sup>102,103</sup> There are also several numerical simulations of ideal relativistic magnetohydrodynamics in the relativistic heavy ion collisions.<sup>104,105</sup> Beyond the ideal fluid, the second order magnetohydrodynamics including the dissipative effects are studied via the Grad's momentum expansion.<sup>106,107</sup> Another macroscopic framework is named Anomalous-Viscous Fluid Dynamics (AVFD),<sup>108–110</sup> where the magnetic fields are considered as the background fields. There are also many studies of the CME in a perturbation aspect of the quantum field theory<sup>111–115</sup> and the chiral charge fluctuation.<sup>116–118</sup> For more discussion on CME and other related topics, one can also see the recent reviews<sup>119–129</sup> and reference therein. Having explored some aspects of the anomaly and the CME, let us explore the Schwinger mechanism, and then we can establish their connection.

### 3. Schwinger Mechanism

In the presence of a strong background electric field, the QFT vacuum is thought unstable against the production of particle anti-particles in what is known as the Schwinger mechanism.<sup>28,130,131</sup> The mechanism had its beginnings as a solution to the Klein paradox,<sup>132</sup> which highlighted the particle non-conserving properties of relativistic QFTs. The Schwinger mechanism may be classified as a QFT instability; others include Hawking radiation,<sup>133</sup> the Unruh effect,<sup>134</sup> pair creation from inflation, e.g., in a Robertson Walker metric, and spontaneous symmetry breaking.<sup>135</sup> Moreover, the Schwinger mechanism may prove indispensable in that it might be used to access such other QFT instabilities; e.g., gravitational effects in Hawking radiation could be mimicked.<sup>136</sup> Schwinger pair production is thought to take place not only in QED but also in Yang-Mills theories,<sup>137–139</sup> and is thought to lead to hadronization stemming from a breaking of chromoelectric flux tubes.

To understand the Schwinger pair production simply, let us make use of a Dirac sea picture. See Fig. 2. It can be seen that under an electric field, with strength  $E$ , that the Dirac spectrum is tilted by  $Ex_3$ , allowing a quantum tunneling of the mass gap that creates a particle anti-particle pair. A characteristic tunneling length must be passed that is proportional to the critical electric field. Not only

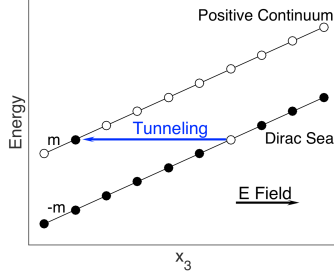


Fig. 2. The Schwinger mechanism in a Dirac sea picture. Dirac spectrum is given for symbolic coordinate,  $x_3$ , the direction of electric field. Excitations (holes) represent particles (anti-particles) whose traversal of the mass gap is made possible owing to the virtue of the electric field, that acts to tilt the spectrum.

from a Dirac sea picture, but also from an intuitive classical perspective can one understand Schwinger pair production. Consider a representation of the vacuum as being composed of virtual particle anti-particle pairs in a condensate, then an electric field may impart work to the pair separating and accelerating them apart.

One may identify a vacuum instability through inequivalent vacuum states at asymptotic times, i.e.,  $\langle \text{in} | \neq \langle \text{out} |$  at  $t_{in}$  and  $t_{out}$  respectively. An S matrix element calculation predicting the vacuum stay the vacuum provides a measure of a vacuum instability, or rather what is more is the calculation predicting anything but the vacuum appear in the out state: It is referred to as the vacuum non-persistence and is given by the probability  $\mathcal{P} := 1 - |\langle \text{out} | \text{in} \rangle|^2$ .  $\langle \text{out} | \text{in} \rangle$  here, confining our attention, is given by the QED partition function in a background field,

$$c_v := \langle \text{out} | \text{in} \rangle = \int \mathcal{D}\bar{\psi} \mathcal{D}\psi \exp \left\{ i \int d^4x [\bar{\psi} (i \not{D} - m) \psi] \right\}. \quad (2)$$

Then casting the partition function as an effective action,  $e^{i\Gamma} := c_v$ , the vacuum non-persistence becomes

$$\mathcal{P} \approx 2\text{Im}\Gamma, \quad (3)$$

for small imaginary parts of  $\Gamma$ . Turning our attention to the Schwinger mechanism, the vacuum non-persistence in a homogeneous electric field with strength,  $E$ , for fermions with mass,  $m$ , is<sup>28</sup>

$$\mathcal{P} \propto \exp \left( \frac{-\pi m^2 c^3}{e E \hbar} \right). \quad (4)$$

Here SI units have been used to highlight the electric field strength required to see Schwinger pair production. Indeed the required field strength is large, in excess of modern capabilities, and therefore the Schwinger mechanism has yet to be observed. But, special temporally inhomogeneous field profiles have shown promise to overcome this difficulty.

Let us digress shortly on “dynamically assisted” fields.<sup>140</sup> Keldysh first found a temporal inhomogeneity in the electric field would lessen the threshold for pair production,<sup>141</sup> effectively relying on a combination of perturbative and non-perturbative components. Then motivated by Keldysh’s work a dynamically assisted combinatory field with both a strong amplitude and low frequency component as well as a weak amplitude and high frequency component was studied, which dramatically improved the probability for pair production.<sup>140, 142–144</sup> The dynamical mechanism and its spin-dependence have also been studied in a perturbative Furry picture,<sup>145–149</sup> as well as numerically.<sup>150</sup> A kinetic theory with usage of the dynamical mechanism,<sup>151</sup> and the momenta spectra<sup>152</sup> were also studied.

Eq. (4) reflects an exponentially quadratic mass suppression, and is the indicative feature of the Schwinger mechanism. In homogeneous fields the factor should be present for observables where the Schwinger mechanism plays a role. Also, let us use Eq. (4) to illustrate the non-perturbative nature of the Schwinger mechanism; this can be seen from the gauge coupling constant  $e$ . Schwinger pair production cannot be seen at any order in perturbation theory. Verification or falsification of the Schwinger mechanism is highly sought and some environments thought capable include condensed matter systems, high powered lasers, and heavy ion collisions.

Condensed matter environments such as for Weyl/Dirac semimetals,<sup>153</sup> semiconductors,<sup>154</sup> or graphene<sup>155, 156</sup> for the potential observation of the Schwinger mechanism are desirable due to a considerably reduced energy gap.<sup>154</sup> In condensed matter environments Schwinger pair production is facilitated through a Landau Zener transition.<sup>157, 158</sup> In place of the positive continuum (Dirac sea) lies the conduction (valence) band. While semimetals and graphene have little or no energy gap, a doped semimetal may possess a tunable gap.<sup>159</sup> Then for gap,  $\Delta$ , one can find for the condensed matter analog the non-persistence probability has the form  $\mathcal{P} \approx \exp(-\frac{\pi\Delta^2}{v_F\hbar eE})$ .<sup>160</sup> In addition to a lessening of the critical field strength, inhomogeneous fields too may prove beneficial,<sup>154</sup> not only in condensed matter but also in QED.

Direct observation of the Schwinger mechanism is theoretically achievable in high powered lasers, and it is an essential task to pursue. Experimentation can be managed with either sole use of lasers or through a laser particle beam collision.<sup>161</sup> Strong QED is actively being studied at numerous high powered laser facilities including the Extreme Light Infrastructure (ELI) and the X-ray Free-Electron Laser Facility (XFEL) in DESY; experimental outlooks are provided in Refs. <sup>136, 162, 163</sup>. However, peak electric fields produced are still order of magnitude, i.e.  $\sim 10^{-2}$ , lower than is the critical electric field required for Schwinger pair production,  $\sim 1.3 \times 10^{18}$  V/m.<sup>164, 165</sup> More so, realistic modeling of high powered laser beams are highly inhomogeneous require numerical modeling; e.g., see Ref. <sup>166</sup>.

On the other hand, the electromagnetic fields generated in relativistic heavy ion collisions are at the order of a few  $m_\pi^2$  with  $m_\pi$  the mass of the pion meson.<sup>167–170</sup> Since the quantum electromagnetic dynamics dominates in the ultra-peripheral col-



lisions (UPC), those experiments may provide a nice and possible platform to study the non-linear effects of QED.<sup>171–175</sup>

With an understanding of the anomaly and Schwinger mechanism in hand, let us examine more closely how chirality may be spawned through pair production.

#### 4. Heuristic Chirality Generation: Anticipations and Challenges

As anticipated earlier fascinating physics emerge with the addition of a parallel magnetic field into an electric field. Whereas the electric field gives rise to produced pairs through the Schwinger mechanism, the magnetic field projects the pairs' spins onto itself producing a net chirality. Let us begin with a cursory look at this process, starting with the Schwinger mechanism in parallel homogeneous fields.

Parallel homogeneous fields allow us to study a parity-violating configuration without being encumbered by technical difficulties. Also, it has been reasoned such fields may give rise to a net chirality through the Schwinger mechanism.<sup>13</sup> The parallel homogeneous fields we use are in the  $x^3$  direction:

$$\vec{B} = B \hat{x}^3, \quad \vec{E} = E \hat{x}^3. \quad (5)$$

The usage of homogeneous fields is just in that in ion-ion collisions, related chromoelectromagnetic flux tubes are thought to form in the glasma.<sup>11,12</sup>

A measure of Schwinger pair production is provided through the imaginary part of the effective action, the vacuum non-persistence, Eq. (3). The relation describing a single particle anti-particle pair is given by <sup>a</sup>

$$2\text{Im}\Gamma \approx Vt\omega, \quad (6)$$

where  $\Gamma$  is the effective action and  $V$  and  $t$  are the volume and time measures of the system.  $\omega$  is the probability that a pair is produced in a given unit space-time. For the case of our homogeneous fields, Eq. (5), Schwinger's formula is famously known as (see e.g., Ref. 178)

$$\omega = \frac{e^2 EB}{4\pi^2} \coth\left(\frac{B}{E}\pi\right) \exp\left(-\frac{\pi m^2}{eE}\right). \quad (7)$$

The Landau levels are contained in the cotangent function, and moreover in the lowest Landau level approximation (LLLA), Schwinger's formula can be seen to resemble the non-conservation of chirality for the chiral anomaly. This is not coincidental we will show throughout this review.

The intuitive picture of chirality generation via the Schwinger mechanism is as follows: Particle anti-particles pairs are spawned from the vacuum from the Schwinger mechanism. And in a strong magnetic field parallel to the electric field,

<sup>a</sup> Note here only the lowest order pole in the effective action is considered to make the single pair interpretation valid. Actually, the probability of a single pair generated is given as a geometric series over all poles,<sup>176</sup> and the imaginary part of the effective action predicts any number of pairs generated from the vacuum. See also Refs. 16, 177

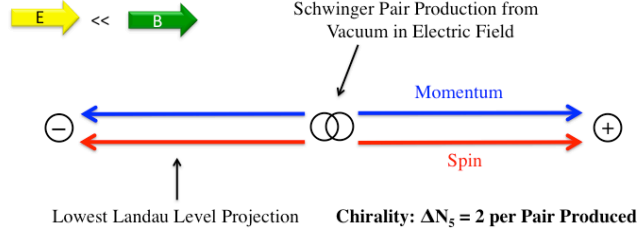


Fig. 3. Cartoon of chirality production from the Schwinger mechanism. A LLLA is taken, and pairs of produced particles will have their spins aligned with the magnetic field, therefore setting up a net chirality,  $\Delta N_5 = 2$ , c.f., Fig. 1.

such that the LLLA may be taken, the particles' spins will be projected to the magnetic field such that a net chirality be generated. In Fig. 3, a cartoon of a produced pair can be seen; there a net chirality of  $\Delta N_5 = 2$  is produced. Also, one needn't assume massless fermions; with only the lowest Landau level being occupied, an effective dimensional reduction will occur, and chirality will be fixed. Let us also digress on the conventions of chirality, as is also outlined in Ref. 4. Massless, or massive in a LLLA, particles with right-handed helicity (spin and momentum are parallel) have right-handed chirality. Whereas anti-particles with left-handed helicity, (spin and momentum are anti-parallel), have right-handed chirality. Therefore  $\Delta N_5$  can be read as the total number of right-handed helicity particles and anti-particles minus the total number of left-handed helicity particles and anti-particles.

We can also benefit from a Dirac sea perspective of the chirality generation process from pair production, as is commonly invoked to explain the Schwinger mechanism. We did so in Fig. 2, however, a coordinate representation was used there. Here we use a momentum representation. A key point in Fig. 2 is that the electric field augments the spectrum, enabling a traversal of the mass gap—a tunneling phenomenon. And an important aspect of the anomaly is a QFT vacuum instability, making possible a non-conservation of chirality.<sup>179</sup>

The energy dispersion relation for massive fermions in parallel fields can be seen in Fig. 4. Again, a LLLA is assumed and hence we have a definite projection of helicity. In the electric field a particle may tunnel from the Dirac sea, leaving an anti-particle in its place. Then due to the strong magnetic field only particles with right-handed chirality and anti-particles with left-handed chirality can be formed; a chirality non-conservation forms as indicated by the axial Ward identity. The infinite Dirac sea supplies particle non-conservation and in turn the anomaly through tunneling. The challenge, we will find, is in the determination of expectation values. Depending on how the vacuum states are constructed, different physics emerges.

Let us quantify the heuristic picture. One may expect for the probability density in unit time of pairs to be produced, in parallel fields, Eq. (7), under the LLLA, to

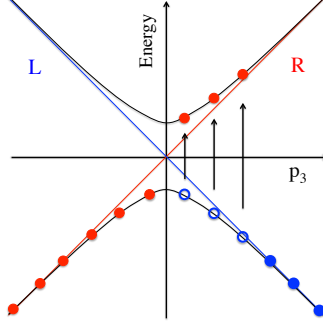


Fig. 4. Dirac sea dispersion relation in momentum space. Dimensional reduction for the massive fermion system is made possible due to the LLLA. Particles tunnel from the Dirac sea leaving anti-particles in their place. Only right-handed particles and left-handed anti-particles are formed, setting up a net chirality.

give rise to the following non-conservation of chiral density:

$$\omega = \frac{e^2 EB}{4\pi^2} \exp\left(-\frac{\pi m^2}{eE}\right) \sim \frac{1}{2} \partial_0 n_5, \quad (8)$$

as illustrated in Ref. 13. Here the chiral density,  $n_5$ , is the expectation value—to later be defined concretely—of the axial current,

$$j_5^\mu := \bar{\psi} \gamma^\mu \gamma_5 \psi. \quad (9)$$

The axial Ward identity is exact at the operator level and reads,

$$\partial_\mu j_5^\mu = -\frac{e^2}{16\pi^2} \epsilon^{\mu\nu\alpha\beta} F_{\mu\nu} F_{\alpha\beta} + 2m \bar{\psi} i \gamma_5 \psi. \quad (10)$$

Then for our field configuration, Eq. (5), we find the expectation value of the above becomes

$$\partial_0 \langle j_5^0 \rangle = \frac{e^2 EB}{2\pi^2} + 2m \langle \bar{\psi} i \gamma_5 \psi \rangle. \quad (11)$$

The discrepancy stems when one performs actual calculation for the above. Notably, Schwinger first performed the calculation of the pseudoscalar condensate in Ref. 28, while studying the neutral meson and proton, to find

$$\bar{P} := \langle \bar{\psi} i \gamma_5 \psi \rangle = -\frac{e^2 EB}{4\pi^2 m}. \quad (12)$$

What is more is that when using the above calculation in the axial Ward identity, Eq. (11), we find  $\partial_0 \langle j_5^0 \rangle = 0$ ! When compared to the heuristic picture, Eq. (8), we find an enigma:

$$n_5 \neq \langle j_5^0 \rangle. \quad (13)$$

This is valid for any  $m$ , including massless fermions. It is often the case that  $m \langle \bar{\psi} i \gamma_5 \psi \rangle$  is dropped for  $m \rightarrow 0$  theories, but we can see here that the step is

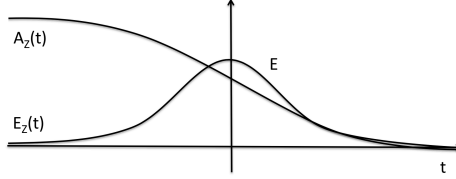


Fig. 5. Sauter potential as an example of an inequivalent vacuum state profile.  $E_z(t) = E \cosh^{-2}(t)$  and  $A_z(t) = -E \tanh(t) + E$ . Note that while the field vanishes at  $t \rightarrow \pm\infty$ , the gauge does not.

unjustified. Let us also point out, massless Abelian theories differ from  $m \rightarrow 0$  theories in that the former has a completely shielded electric charge.<sup>180</sup> A resolution to the above enigma, we will demonstrate, can be had with an identification of vacuum states. Depending on the makeup of the vacuum states, expectation values can differ markedly, both quantitatively and through physical interpretation.

## 5. Vacuum States and Expectation Values

There are implications for expectation values derived from fields and their gauges whose behavior differs at asymptotic times. This is even the case, for example, for the Sauter potential.<sup>130</sup> Note that we, rather, use homogeneous fields throughout this review. Even though the field disappears in the asymptotic limits the gauge does not; see Fig. 5. If then the background field differs at its asymptotic limits, then the corresponding vacuum states too are affected. This leads to a vacuum instability, and for the case of a background electric field, manifests itself as the Schwinger mechanism. The differing vacuum states are characterized as  $|\text{in}\rangle \neq |\text{out}\rangle$ . Naïve usage of vacuum states under a vacuum instability in the calculation of expectation values may lead to physical interpretations being marred. This we will show was the case for the pseudoscalar condensate, Eq. (12). Let us emphasize, there is nothing wrong with the calculation leading to Eq. (12). In fact, its physical interpretation is profound, we will show. But, how might one calculate values in accordance with our heuristic understanding? This is accomplished by noting that the Schwinger mechanism is an inherently out-of equilibrium phenomenon. And as such, calculations therein can only be had with techniques with out-of equilibrium capacity. The in-in formalism<sup>176</sup> provides a means. The formalism's usage is intuitive as well in that expectation values are manifestly real and coincide with quantum mechanical expectation value definition.

We employ two vacuum state expectation value types throughout this review, both the conventional in-out and in-in types, which we contrast for operator,  $\mathcal{O}(t)$ , as

$$\langle \mathcal{O} \rangle := \langle \text{out} | \mathcal{O}(t) | \text{in} \rangle / c_v, \quad \langle\langle \mathcal{O} \rangle\rangle := \langle \text{in} | \mathcal{O}(t) | \text{in} \rangle, \quad (14)$$

where the  $c_v$  is defined in Eq. (2). Here we emphasize again that the in and out vac-

uum states are defined at asymptotic times  $t_{in} \rightarrow -\infty$  and  $t_{out} \rightarrow \infty$  respectively.

One may expand Dirac operators, conveniently if they wish, at the asymptotic times with creation and annihilation operators acting on the respective vacuum state. We expanded the wave function as,

$$\begin{aligned}\psi(x) &= \sum_n a_n^{in} \phi_{+n}^{in}(x) + b_n^{in\dagger} \phi_{-n}^{in}(x) \\ &= \sum_n a_n^{out} \phi_{+n}^{out}(x) + b_n^{out\dagger} \phi_{-n}^{out}(x).\end{aligned}\quad (15)$$

where  $\phi_{+n}$  ( $\phi_{-n}$ ) depicts an eigenvector of the Dirac equation with a positive (negative) energy solution and eigenvalue,  $n$ . Both the in and out representations are valid over all times. The creation and annihilation operators, for example in the in basis, act such that

$$a_n^{in} |in\rangle = b_n^{in} |in\rangle = \langle in| a_n^{in\dagger} = \langle in| b_n^{in\dagger} = 0, \quad (16)$$

with the usual anti-commutation relations applying:  $\{a_n^{in}, a_m^{in\dagger}\} = \{b_n^{in}, b_m^{in\dagger}\} = \delta_{nm}$ . One may construct a similar set for the out basis as well.

For the calculation of expectation values indicated in Eq. (14), we introduce two useful respective causal propagators

$$S^c(x, y) = i \langle T \psi(x) \bar{\psi}(y) \rangle, \quad (17)$$

$$S_{in}^c(x, y) = i \langle \langle T \psi(x) \bar{\psi}(y) \rangle \rangle. \quad (18)$$

While both of the propagators satisfy a similar differential equation,

$$-(i \not{D}_x - m) S_{\text{null}, in}^c(x, y) = \delta(x - y), \quad (19)$$

their boundary conditions and behavior differ.

### 5.1. In-Out Propagator

Let us examine first the more conventional in-out propagator. As illustrated with the above arguments, expectation values sought using the in-out propagator correspond to a matrix element with ground states at asymptotic times, i.e.,  $x^0 \rightarrow \pm\infty$ . The meaning of such observables is fascinating in its own right and thus we elaborate in some depth later; here in this section, however, we confine our attention to the derivation of the in-out propagator.

The in-out propagator is defined from a matrix element for asymptotic in to out states, and reads in path integral form as

$$S^c(x, y) = \int \mathcal{D}\bar{\psi} \mathcal{D}\psi \psi(x) \bar{\psi}(y) \exp \left\{ i \int d^4x' \bar{\psi}(i \not{D} - m) \psi \right\}. \quad (20)$$

In contrast to the in-in propagator for inequivalent vacuum states<sup>b</sup>, the above per-

<sup>b</sup>For equivalent vacuum states the in-out and in-in propagators coincide.

mits a formal but simple functional representation in proper time:

$$S^c(x, y) = \langle x | \frac{-1}{i\hat{\mathcal{D}} - m} | y \rangle = (i\hat{\mathcal{D}}_x + m) \langle x | \frac{1}{\hat{\mathcal{D}}^2 + m^2} | y \rangle. \quad (21)$$

Hats, (e.g.  $\hat{\mathcal{O}}$ ), denote operators, and are acted upon by states in 3+1 spacetime denoted with brackets. We also stress there is a small imaginary piece implicit in the mass term,  $m^2 \rightarrow m^2 - i\epsilon$ , that is left out for brevity. The small imaginary piece dictates the time ordering and also guarantees convergence in the infrared limit.

The connection to Schwinger proper time<sup>28 c</sup> is accomplished with a Laplace transform,

$$\hat{\mathcal{O}}^{-1} = i \int_0^\infty ds \exp(-i\hat{\mathcal{O}}s), \quad (22)$$

with  $s$  representing a proper time-like parameter. Using Eq. (21) one can find

$$S^c(x, y) = (i\hat{\mathcal{D}}_x + m) \int_0^\infty ds g(x, y, s), \quad (23)$$

$$g(x, y, s) := i \langle x | e^{-i\hat{H}s} | y \rangle, \quad (24)$$

$$\hat{H} := \hat{\mathcal{D}}^2 + m^2, \quad (25)$$

for kernel,  $g$  and proper time Hamiltonian,  $\hat{H}$ . It is convenient to express the kernel in its path integral form, and this is easily done by finding the accompanying Lagrangian,  $\mathcal{L}$ , for the Hamiltonian, and also through the use of the identity

$$\langle x | e^{-i\hat{H}s} | y \rangle = \int_{x(0)=y}^{x(s)=x} \mathcal{D}x \mathcal{P} e^{i \int_0^s d\tau \mathcal{L}}. \quad (26)$$

We can find the Lagrangian through a Legendre transform,<sup>183</sup> where operators in Heisenberg notation,  $\hat{\mathcal{O}}(\tau)$ , follow Heisenberg equations of motion in proper time,  $\tau$ , as

$$\dot{\hat{\mathcal{O}}} := \frac{d\hat{\mathcal{O}}}{d\tau} = -i[\hat{\mathcal{O}}, \hat{H}]. \quad (27)$$

The canonical commutation relations read  $[\hat{p}_\mu, \hat{x}_\nu] = i g_{\mu\nu}$ . Then using Eq. (25), we can find the velocity as  $\dot{\hat{x}}_\mu = 2(\hat{p}_\mu - eA_\mu(\hat{x}))$ . And the Lagrangian from the Legendre transformation,  $\hat{\mathcal{L}} = \hat{p}_\mu \frac{\partial \hat{H}}{\partial \hat{p}^\mu} - \hat{H}$ , is

$$\hat{\mathcal{L}} = -\frac{1}{4}\dot{\hat{x}}^2 - eA(\hat{x})\dot{\hat{x}} - \frac{e}{2}F(\hat{x})\sigma - m^2, \quad (28)$$

where we have used a contracted notation for the Lorentz indices, e.g.  $F\sigma = F^{\mu\nu}\sigma_{\mu\nu}$  with  $F^{\mu\nu}$  being the field strength tensor and  $\sigma^{\mu\nu} := \frac{i}{2}[\gamma^\mu, \gamma^\nu]$ . Finally the kernel in path integral form using Eq. (26) is identified as

$$g(x, y, s) = i \int_{x(0)=y}^{x(s)=x} \mathcal{D}x \mathcal{P} \exp \left\{ i \int_0^s d\tau \left[ -\frac{1}{4}\dot{x}^2 - eA\dot{x} - \frac{e}{2}F\sigma - m^2 \right] \right\}, \quad (29)$$

<sup>c</sup>For path integral representations of Schwinger proper time see Refs. 181, 182

where  $\mathcal{P}$  indicates time-ordering for proper time  $\tau$ . This is the kernel of the worldline path integral<sup>184,185</sup> and while the above form is valid for any background QED field, at this point let us restrict our attention to the case of parallel electric and magnetic fields, Eq. (5). The in-out propagator in homogeneous parallel fields is a well-known expression,<sup>28,183</sup> however steps worked through in its derivation will aid in later discussions.

For homogeneous fields we can factorize the kernel into both a spin factor  $\Phi(s)$  and boson path integral  $b(s)$  such that they are connected through proper time as in

$$g(s) = b(s)\Phi(s)\exp(-im^2s), \quad (30)$$

with

$$b(x, y, s) := \int_{x(0)=y}^{x(s)=x} \mathcal{D}x \exp\left\{i \int_0^s d\tau \left[-\frac{1}{4}\dot{x}^2 - eA\dot{x}\right]\right\}, \quad (31)$$

$$\Phi(s) := \mathcal{P} \exp\left\{-i \int_0^s d\tau \frac{e}{2} F \sigma\right\}. \quad (32)$$

We first address the spin factor. For our choice of fields in the  $x^3$  direction and with the use of Weyl gamma matrices, Eq. (1), the spin factor takes a diagonal form. The path ordering is negated simplifying matters. Here we represent the spin factor using gamma matrices as

$$\Phi(s) = [\cos(eBs) + i \sin(eBs)\sigma^{12}] \times [\cosh(sEs) + \sinh(eEs)\gamma_5\sigma^{12}], \quad (33)$$

with  $\sigma^{12} = \text{diag}[1, -1, 1, -1]$ . Then all that is needed to solve the in-out propagator is to determine the boson path integral.

In homogeneous fields the boson path integral, Eq. (31), has an exact solution in steepest descents owing to the quadratic form of coordinates in the action. We use the Fock-Schwinger gauge,

$$A_\mu(x) = -\frac{1}{2}F_{\mu\nu}x^\nu. \quad (34)$$

We can evaluate the path integral though steepest descents; we expand  $x$  about the classical path,  $x^{cl}$ , such that  $x_\mu(\tau) = x_\mu^{cl} + \eta_\mu(\tau)$ . for small fluctuations,  $\eta$ . The fluctuations disappear at the endpoints,  $\eta(0) = \eta(s) = 0$ . Then for the worldline action,  $S_b = \int_0^s d\tau [-\frac{1}{4}\dot{x}^2 - eA\dot{x}]$ , one can find Eq. (31) becomes

$$b(x, y, s) = e^{iS_b(x^{cl})} \mathcal{F}, \quad (35)$$

$$\mathcal{F} := \int \mathcal{D}\eta \exp\left\{i \int_0^s d\tau \left[-\frac{1}{4}\dot{\eta}^2 + \frac{1}{2}\eta eF\dot{\eta}\right]\right\}. \quad (36)$$

The classical equation of motion for the boson worldline action is simply the Lorentz force equation

$$\ddot{x}^{cl\mu}(\tau) = 2eF_{\nu}^{\mu}\dot{x}^{cl\nu}(\tau), \quad (37)$$

with solution,  $\dot{x}^{cl\mu}(\tau) = [e^{2eF\tau}]^\mu_\nu \dot{x}^{cl\nu}(0)$ . Then for the displacement

$$z := x - y, \quad (38)$$

and taking note of the boundary conditions for the boson path integral one can find that  $\int_0^s d\tau \dot{x}^{cl\mu}(\tau) = z^\mu$ . Also it can be found that  $(e^{2Fs} - 1)^\mu_\lambda \dot{x}^{cl\lambda}(0) = 2F^\mu_\lambda z^\lambda$ . Last, using the above relationships one can find the for the classical worldline action

$$\varphi := S_b(x^{cl}) = \frac{1}{2} x eF y - \frac{1}{4} z \coth(eFs) eF z \quad (39)$$

$$= \frac{1}{2} x eF y + \frac{1}{4} [(z_3^2 - z_0^2) eE \coth(eEs) + (z_1^2 + z_2^2) eB \cot(eBs)]. \quad (40)$$

Let us point out that all the gauge dependence resides in the  $x eF y$  term, and also that after application of the covariant derivative acting on the kernel, the classical worldline action vanishes as  $x \rightarrow y$ .

One may calculate the fluctuation prefactor, Eq. (36), by expanding about Fourier modes, i.e.:

$$\eta_\mu(\tau) = a_{\mu 0} + \sum_{n=1}^{\infty} \left[ a_{\mu n} \cos\left(\frac{2\pi n\tau}{s}\right) + b_{\mu n} \sin\left(\frac{2\pi n\tau}{s}\right) \right]. \quad (41)$$

After some steps, and equipped with the free field solution,

$$\int \mathcal{D}\eta e^{i \int_0^s d\tau [-\frac{1}{4} \dot{\eta}^2]} = -i/(4\pi s)^2, \quad (42)$$

it can be found the fluctuation prefactor becomes

$$\mathcal{F} = -i \frac{e^2 EB}{(4\pi)^2} \sin^{-1}(eBs) \sinh^{-1}(sEs). \quad (43)$$

Finally, we may gather all the terms to find the kernel, Eq. (24), as

$$g(x, y, s) = \frac{e^2 EB}{(4\pi)^2} \frac{\exp[-im^2 s + i\varphi(x, y, s)]}{\sin(eBs) \sinh(eEs)} \Phi(s), \quad (44)$$

with spin factor given in Eq. (33). Using proper time methods we have at our disposal a wealth of physics described in a compact expression. All the physics of the Schwinger mechanism is contained in the kernel. Let us illustrate that by making the connection to Schwinger's formula, Eq. (7). The effective action may be expressed as

$$\Gamma[A] = -i \text{Tr} \ln(i\mathcal{D} - m) \quad (45)$$

$$= \frac{1}{2} \text{tr} \int d^4x \int_0^\infty \frac{ds}{s} g(x, x, s). \quad (46)$$

Then evaluating for the imaginary part, taking only the contribution of the lowest order pole at  $s = -\pi/eE$ , and using Eq. (6), one can find Schwinger's formula, Eq. (7). Also, all the spin structure of the system is contained in the spin factor. And last, all the Landau levels are kept in the  $\cot(eBs)$  functions. The kernel and the in-out propagator are exact to one loop. For extensions to QCD see Ref.<sup>186</sup> The in-in propagator may be cast in a similar form, in fact with just a modification to the proper time integral in  $s$ .



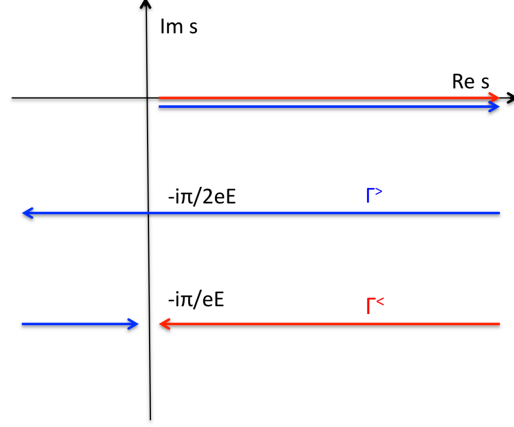


Fig. 6. In-in propagator contours in proper time,  $s$ .  $\Gamma^>$  and  $\Gamma^<$  are valid for positive and negative  $z_3$  respectively. Contours near the real axis lie slightly below it.

## 5.2. In-In Propagator

The proper time representation of the in-out propagator is compact and it would be advantageous to do the same for the in-in propagator. This has fortunately been accomplished by Fradkin et. al. in Ref. 176, and they find the only modification of which in comparison to the in-out case is an augmentation of the proper time integral.

There it is found the in-in propagator can be cast into a Schwinger proper time representation, where the in-out contour has been subsumed into the overall contour, as

$$S_{\text{in}}^c(x, y) = (i\not{D}_x + m) \int_{\text{in}} ds g(x, y, s) \quad (47)$$

$$\int_{\text{in}} ds := \left[ \theta(z_3) \int_{\Gamma^>} ds + \theta(-z_3) \int_{\Gamma^<} ds \right]. \quad (48)$$

The contours are given in Fig. 6. We have acquired Heaviside theta function arguments in the proper time integral and kernel. The arguments are important in that they give rise to the real-time dependence in our out-of equilibrium formulation. We further illustrate their nature with concrete examples in the coming sections.

Recently, we have found the deep connection between the in-in propagator in Eq. (48) and famous Schwinger-Keldysh (closed-time-path) formalism.<sup>187, 188</sup> We can also derive the Eq. (48) through the analyzing the Bogoliubov coefficients of in and out states<sup>176</sup>. We will present these results somewhere else. We have introduced both the in-out and in-in formalisms, and now let us examine their differences and characteristics.

### 5.3. In-Out and In-In Expectation Values

Let us consider a Wick rotation of the Lagrangian, e.g., as provided in Eq. (2), such that  $x^0 = -ix^4$ . Naturally, this describes a Euclidean QFT at zero temperature, with action  $\int_0^\beta dx^4 \int d^3x [\bar{\psi}(i\mathcal{D} - m)\psi]$ , and hence in equilibrium. And thus in-out observables should correspond to a Euclidean equilibrium picture. Furthermore, owing to the periodicity of Euclidean time, the Euclidean partition function and hence its vacuum states too ought to follow periodicity, i.e.,  $\langle x_{in}^4 = 0 | = \langle x_{out}^4 = \beta |$ . In spite of the above straightforward arguments, an interpretation of Euclidean equilibrium for in-out observables has subtleties.

A merit of the in-in or Schwinger-Keldysh formalism is the guarantee of real observables for single bilinear fermion fields provided through the Hermiticity of their construction. This, however, is not the case for in-out observables; there one can find  $\langle \bar{\psi}\mathcal{O}\psi \rangle \neq \langle \bar{\psi}\mathcal{O}\psi \rangle^*$ , even for certain Hermitian  $\mathcal{O}$ . And we will show with a concrete example imaginary pieces can reside in in-out observables. This problem is present in cosmological applications as well, where an in-out construction may give way to a complex metric, making physical interpretation challenging.<sup>189</sup> The source of the problem stems from a Wick rotation under an electric field. Strictly speaking, a Euclidean QFT is defined under  $U_A(1)$  with all fields real—and hence complex in Minkowski space. In our case, we began with all real fields in Minkowski space then after a Wick rotation one would find complex fields in Euclidean space; thus enlarging the gauge group. Indeed, an imaginary electric field in Euclidean space is generally utilized in the study of Schwinger pair production.<sup>190,191</sup> And more generally the sign problem, as is readily the case in a Euclidean metric, is a necessary ingredient for Schwinger pair production to occur. Despite the above reasoning, for the most physically relevant observables, outlined below, no imaginary piece is found and therefore the interpretation of Euclidean equilibrium holds. And for any case, that the in-out formalism not predict any produced pairs in the out state always holds. Having both the in-out and in-in propagator at our disposal, let us proceed with the evaluation of chiral related expectation values.

## 6. Axial Ward Identity

Having determined the importance of vacuum states in the determination of expectation values, and their (out-of) equilibrium nature, let us proceed with concrete calculations. We begin with the enigma, Eq. (13), or rather the axial Ward identity, Eq. (11). We will illustrate how the controversy is solved using Schwinger proper time methods both in and out-of equilibrium as discussed in previous sections. The determination of the axial Ward identity in homogeneous fields is entirely dictated by the pseudoscalar condensate term. This is because  $\langle \epsilon^{\mu\nu\alpha\beta} F_{\mu\nu} F_{\alpha\beta} \rangle = \langle\langle \epsilon^{\mu\nu\alpha\beta} F_{\mu\nu} F_{\alpha\beta} \rangle\rangle = \epsilon^{\mu\nu\alpha\beta} F_{\mu\nu} F_{\alpha\beta}$ .

We first address the equilibrium or in-out pseudoscalar condensate. The result was written above without proof in Eq. (12). Here, let us examine the quantity in the context of Schwinger proper time. And, indeed Schwinger was the first to examine

the pseudoscalar condensate through such means.<sup>28</sup> Using the in-out propagator, Eq. (21), we have the compact expression for the pseudoscalar condensate in parallel homogeneous fields, Eq. (5),

$$\bar{P} := \langle \bar{\psi} i \gamma_5 \psi \rangle = - \lim_{y \rightarrow x} \text{tr}[\gamma_5 S^c(x, y)]. \quad (49)$$

Evaluation of the above can be readily done. Let us begin by noting that the portion of the covariant derivative,  $\not{D}$  acting on the kernel,  $g$ , in  $S^c$  vanish owing to the fact that an odd number of gamma matrices vanish under a trace. In fact, we will find more generally that this term vanishes for point split expectation values due to translational symmetry, i.e.,  $g(x, y) = g(x - y)$ . For the remaining mass dependent term in the pseudoscalar condensate we also find a cancellation from the term of the spin factor, after taking the Dirac trace, and the boson path integral fluctuation term. The remaining form reads

$$\bar{P} = - \lim_{y \rightarrow x} 4i \frac{me^2 EB}{(4\pi)^2} \int_0^\infty ds e^{-im^2 s + i\varphi(x, y, s)} = - \frac{e^2 EB}{4\pi^2 m}. \quad (50)$$

Even despite the essential singularity in  $\varphi$ , after taking the  $x \rightarrow y$  limit all terms with  $z$  dependence vanish; we will show this step shortly. Using the above and Eq. (11), one can find that the axial Ward identity

$$\partial_0 \bar{n}_5 := \partial_0 \langle \bar{\psi} \gamma^0 \gamma_5 \psi \rangle = 0, \quad (51)$$

predicts a conservation of chirality for any mass. It is quite astonishing that this should be the case. We will find that the enigma and the above relationship are resolved using an in-in, or out-of equilibrium, formalism. And thus, the chiral anomaly persists as expected; see Eq. (8). However, we find here in Euclidean equilibrium no such non-conservation, suggesting the anomaly only exist out-of equilibrium. One may anticipate such a scenario in the context of a condensed matter system for the CME, a close relative of the anomaly. There the disappearance of the CME in equilibrium, but its reemergence out-of equilibrium is well-known.<sup>192</sup> And the same phenomenon is echoed here for the anomaly. One can see why Eq. (51) should hold for the massless case: Topological properties are independent of a  $\theta$  term and hence a nonzero topological charge or net chirality would not be expected.

Eq. (51) is valid for any mass and thus the pseudoscalar term should always be kept, even for small masses in QED and QCD. However, one may discover the effects of a mass on the axial Ward identity through the use of nonequilibrium techniques. Also, in doing so, we can resolve the enigma and show the dependence of the chiral anomaly on the Schwinger mechanism. To reiterate, in-out, or Euclidean equilibrium, expectation values predict no pairs of particles in the out state generated via the Schwinger mechanism, whereas in-in, or out-of equilibrium, expectation values predict any number of pairs.

In analogy to the in-out case, Eq. (49), let us directly calculate the out-of equilibrium pseudoscalar condensate using the in-in propagator, Eq. (48),

$$P := \langle \langle \bar{\psi} i \gamma_5 \psi \rangle \rangle = - \lim_{y \rightarrow x} \text{tr}[\gamma_5 S_{\text{in}}^c(x, y)]$$

$$= -\lim_{y \rightarrow x} i \frac{me^2 EB}{4\pi^2} \left[ \theta(z_3) \int_{\Gamma^>} + \theta(-z_3) \int_{\Gamma^<} \right] ds e^{-im^2 s + i\varphi(x, y, s)}, \quad (52)$$

where we have repeated similar steps as were taken in the Euclidean equilibrium case above. One may actually evaluate the above for either  $z_3 \rightarrow \pm 0$  and hence either  $\Gamma^>$  or  $\Gamma^<$ , and this is due to the fact that the pseudoscalar condensate is unaffected by a point-splitting scheme. We elect to use conventions as written in Sec. 1. Then one may deform the contours to obtain for the in-in pseudoscalar condensate,<sup>21</sup>

$$\begin{aligned} P &= -4i \frac{me^2 EB}{(4\pi)^2} \left[ \int_0^\infty ds - \int_{-i\frac{\pi}{eE}}^{\infty - i\frac{\pi}{eE}} ds \right] e^{-im^2 s} \\ &= -\frac{e^2 EB}{4\pi^2 m} \left[ 1 - \exp\left(-\frac{\pi m^2}{eE}\right) \right], \end{aligned} \quad (53)$$

in agreement with the heuristic expression, Eq. (8). Note that the rigorous way to evaluate Eq. (52) is to integrate over  $\Gamma^>$  and  $\Gamma^<$  first and then take the  $z_3 \rightarrow 0$  limit as we will show in a later calculation of  $j_5^\mu$ .

Chirality has been generated through the Schwinger mechanism. Likewise, using Eq. (11), one can find for the in-in out-of equilibrium axial Ward identity,

$$\partial_0 n_5 := \partial_0 \langle \bar{\psi} \gamma^0 \gamma_5 \psi \rangle = \frac{e^2 EB}{2\pi^2} \exp\left(-\frac{\pi m^2}{eE}\right). \quad (54)$$

We have recovered the chiral anomaly, and also shown its dependence on mass. We also find that only the Schwinger mechanism has contributed to the non-conservation of chirality. We also point out that Eq. (53) was also inferred from the axial Ward identity in Ref. 15.

It is also interesting to draw the connection between the proper time formalism and the Fujikawa<sup>193</sup> method, so we digress here. The Fujikawa method entails that the anomaly arises from the QFT path integral measure after performing a chiral rotation. The method predicts the anomaly despite usage of massless fermions. Important in the Fujikawa method is the careful regularization of the functional trace of  $\gamma_5$ . And, in fact, this same heat-kernel regularization process is present in the Schwinger proper time construction: It is the ultraviolet, or small  $s$ , limit.

It is instructive to confirm our previous results on the axial Ward identity by directly calculating the chiral density. Doing so, we will find, provides insight into the real-time nature of our out-of equilibrium observables. As before, however, let us address the Euclidean equilibrium case first; the chiral current, with  $\bar{n}_5$  being the density, is in proper time notation

$$\bar{j}_5^\mu := \langle \bar{\psi} \gamma^\mu \gamma_5 \psi \rangle = i \lim_{y \rightarrow x} \text{tr}[\gamma^\mu \gamma_5 S^c(x, y)]. \quad (55)$$

Such a term we can show for our fields, Eq. (5), vanishes, and is therefore in agreement with Eq. (51). Noting again that the trace of an odd number of Dirac matrices vanishes we can see that only the covariant derivative piece remains,

$$\bar{j}_5^\mu = -i \lim_{y \rightarrow x} \text{tr}[\gamma^\mu \gamma_5 \not{D}_x \int_0^\infty ds g(x, y, s)]. \quad (56)$$

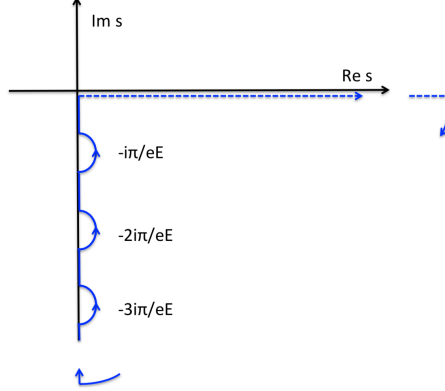


Fig. 7. Proper time contour rearrangement using Cauchy's integral theorem to imaginary values. Convergence is provided by the  $m^2 - i\epsilon$  term. Singularities can be found at  $s = -i\frac{n\pi}{eE}$  for  $n = 1, 2, \dots$

It is known that in homogeneous fields such a term should be zero; see e.g. Refs. 176, 194, and this is because of translational symmetry. However, let us show why it should be the case. Allowing the covariant derivative act on the kernel one can find

$$\begin{aligned} \not{D}_x g(x, y, s) &= (\partial_\mu - \frac{i}{2} e F_{\mu\nu} x^\nu) \gamma^\mu g(x, y, s) \\ &= -\frac{1}{2} \left[ i e F_{\mu\nu} + (\coth(eFs) eF)_{\mu\nu} \right] z^\nu \gamma^\mu g(z, s), \end{aligned} \quad (57)$$

and hence a factor  $z$  is present. Then so long as the kernel be analytic as  $x \rightarrow y$ , Eq. (57) should go to zero as  $x \rightarrow y$ . Outside of the singularities this will clearly be the case, however near the singularities we expand about the poles and then take the limit. Note, we have defined the Schwinger proper time contour so that it lies slightly below the real axis. The singularities in the kernel,  $g$ , can be seen in Fig. 7; where we have rotated the contour to imaginary  $s$ . There are essential singularities at  $-i\frac{n\pi}{eE}$  for  $n = 1, 2, \dots$  in  $\varphi$  enclosed in semicircle contours. We expand about the poles and apply the following residue formula for pole  $n$  for their treatment:

$$-i\pi \text{Res}\left(g, -i\frac{n\pi}{eE}\right) = \frac{-i\pi}{(n-1)!} \lim_{s \rightarrow 0} \frac{d^{n-1}}{ds^{n-1}} \left[ \left(s + \frac{in\pi}{eE}\right) g(s) \right]. \quad (58)$$

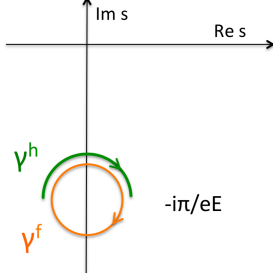
However, with the application of the covariant derivative and upon taking the  $x \rightarrow y$  limit one can find

$$\lim_{y \rightarrow x} \not{D}_x \text{Res}\left(g, -i\frac{n\pi}{eE}\right) = 0. \quad (59)$$

Therefore, we find that the Euclidean equilibrium chiral density,  $\bar{j}_5^\mu$ , vanishes and thus is in agreement with Eq. (51) and the vanishing of the anomaly in equilibrium. However, as anticipated earlier the out-of equilibrium chiral density does not vanish.

The in-in, or out-of equilibrium, chiral density is

$$j_5^\mu := \langle\langle \bar{\psi} \gamma^\mu \gamma^5 \psi \rangle\rangle = i \lim_{y \rightarrow x} \text{tr}[\gamma^\mu \gamma_5 S_{in}^c(x, y)]. \quad (60)$$

Fig. 8. Various contours in proper time,  $s$ , used throughout.

Observing that the trace of an odd number of gamma matrices vanishes,

$$j_5^\mu = -i \lim_{y \rightarrow x} \text{tr}[\gamma^\mu \gamma_5 \not{D}_x \int_{in} ds g(x, y, s)]. \quad (61)$$

We find the key difference with the in-in formalism and Eq. (56) is an augmentation of the proper time contour to include  $\theta(\pm z_3)$ . Whereas before, Eq. (59), we found that the kernel, after being acted on by a covariant derivative and  $x \rightarrow y$  limit, vanished, here we find real-time dependence arises from a phase space factor. Let us rearrange the proper time contours given above for both  $\Gamma^<$  and  $\Gamma^>$  as done in Fig. 7; what remains is a semicircle contour about  $s = -i\pi/eE$ . We denote the semicircle contour as  $\int_{\gamma^h}$ ; see Fig. 8 for the semicircle, as well as other contours used later. In contrast to the Euclidean equilibrium case, we find certain residues do not disappear after taking the  $x \rightarrow y$  limit. Let us illustrate that fact with a sample encountered integral:

$$I_h = \int_{\gamma^h} ds e^{-im^2 s + i\varphi(x, y, s)} \coth(eEs). \quad (62)$$

We first shift the proper time argument such that  $s \rightarrow s' + \frac{i\pi}{eE}$  and keep only leading terms in  $z$  for small  $z$  in the integrand, to find

$$I_h \approx e^{-\frac{m^2\pi}{eE}} \int_{\gamma^h + i\frac{\pi}{eE}} \frac{ds}{eEs} e^{-\frac{i}{4s}(z_0^2 - z_3^2)} \quad (63)$$

$$= e^{-\frac{m^2\pi}{eE}} \int_{-\infty}^{\infty} \frac{d\eta}{eE\eta} e^{-\frac{i}{4}(z_0^2 - z_3^2)\eta} = -\frac{2\pi i}{eE} \theta(z_3^2 - z_0^2) e^{-\frac{m^2\pi}{eE}} \quad (64)$$

where in the second step we have made the change of variables,  $\eta = 1/s$ , leading to a Heaviside function. One may perform a similar set of computations to find integrals without the  $\coth(eEs)$  factor in the integrand, from the spin factor, Eq. (33), vanish in the  $x \rightarrow y$  limit. Let us also mention in passing that one could also use the relation for the singularity,  $\int_{\gamma^h} ds g = \theta(z_3^2 - z_0^2) \int_{\gamma^f} ds g$ , and the residue formula, Eq. (58) to find Eq. (64); see Fig. 8. Returning to  $j_5^\mu$ , let us take the Dirac trace and keep terms with a  $\cosh(eEs)$  in the spin factor, (and hence  $\coth(eEs)$  factor when combined

with the boson path integral factor), as dictated above. We find for the Dirac trace

$$\begin{aligned} \text{tr } \gamma_0 \gamma_5 \not{D} \exp\left(-\frac{i}{2} e F \sigma s\right) &= D_\nu \left[ i \sin(eBs) \cosh(eEs) \text{tr}(\gamma_0 \gamma_5 \gamma^\nu \sigma^{12}) \right. \\ &\quad \left. - \frac{1}{2} \sin(eBs) \sinh(eEs) \text{tr}(\gamma_0 \gamma_5 \gamma^\nu \gamma_5 \sigma^{12}) + \cos(eBs) \sinh(eEs) \text{tr}(\gamma_0 \gamma_5 \gamma^\nu \gamma_5 \sigma^{12}) \right]. \end{aligned} \quad (65)$$

Keeping the relevant terms in the spin factor, and closing the contours in  $\Gamma^<$  and  $\Gamma^>$ , we find for Eq. (61),

$$j_5^\mu = \lim_{x \rightarrow y} i \frac{e^2 EB}{4\pi^2} \partial^3 \theta(z_3) I_h(z) \delta_3^\mu. \quad (66)$$

Let us pause the above calculation to digress on the emergence of real-time. This in fact stems from the  $\theta(\pm z_3)$  terms in  $\int_{in}$ . When acted upon by the partial derivative the resulting delta function is a measure of the phase space in our system and real-time,  $t$ , dependence:<sup>176, 195</sup>

$$\lim_{y \rightarrow x} \delta(z_3) = \lim_{y \rightarrow x} \int \frac{dp_3}{2\pi} e^{ip^3 z^3} = \frac{eEt}{2\pi}. \quad (67)$$

Such an identification is just; we can approach this through both an examination of the canonical and kinetic momenta differences,<sup>196</sup> and also through a look at the Dirac equation.<sup>197</sup> For the former, let us consider a wavepacket perspective. A magnetic field and hence electric field will give harmonic oscillator solutions to the Dirac equation. For the electric fields, the wavepacket would have its solutions in time shifted by the canonical momentum,  $p_3/eE$ , and also energies would be independent of  $p_3$ . Then assuming for some initial time the kinetic momentum of the produced pairs would be zero would imply  $p_3 = eEt$ , which gives  $t$  as a total time measure of the system. One could then anticipate an integration over all canonical momentum as being analogous to one over all time. However in this argument, and also as it pertains to Eq. (67), one must emphasize that a picture of particle production is valid at any time. We can see this in the fact that solutions of the Dirac equation, are in fact valid at any time, not just in the out (or in) asymptotic states.<sup>196</sup> Therefore, Eq. (67) is only valid for operators evaluated at an asymptotic time, i.e.,  $a_n^{out, in}, b_n^{out, in}$ .

In an asymptotic state expansion of the Dirac equation in an electric field—or with parallel magnetic field—one encounters a parabolic cylinder function with time dependence,<sup>197</sup> e.g.,  $D_{a-1}[\sqrt{eE}^{-1}(1-i)(p_3 - eEx_0)]$ , for complex coefficient  $a$ . The complex parabolic cylinder functions have distinct particle and anti-particle pictures at asymptotic times. Let's take for example one with a particle identification at  $x_0 \rightarrow \infty$ . Taking the same solution but at  $x_0 \rightarrow -\infty$ , one can see an admixture of particle and antiparticle states. Therefore, one can indicate a time intervals in which the particle and antiparticle states are fully defined.<sup>197</sup> This time interval is centered about  $x_0 = p_3/eE$  in the above, revealing when pair production occurs. See Ref.<sup>197</sup> for further details.

Finally, using Eq. (67) and carefully evaluating the Heaviside function arguments using notations given in Sec. 1 one can find for the in-in real-time chiral density from the Schwinger mechanism as,<sup>15,21</sup>

$$j_5^\mu = \frac{e^2 E B t}{2\pi^2} \exp\left(-\frac{\pi m^2}{eE}\right) \delta_3^\mu, \quad (68)$$

in agreement with the pseudoscalar and axial Ward identity calculations given in Eqs. (53) and (54) respectively. Let us also point out that the chirality production via the Schwinger mechanism has been extended to dynamically assisted configurations enhancing the rate of chirality production.<sup>147</sup>

## 7. Chiral Magnetic Effect Current

We have established the role the Schwinger mechanism plays on the chiral anomaly through the axial Ward identity above, and it would be instructive to examine the CME as well. As expected similar behavior exists for the CME and chiral vector current in homogeneous fields. As advertised in Sec. 1 and as argued in Ref. 13, there is no need for artificial placement of a chiral chemical potential to see the CME. Let us demonstrate that here and in so doing confirm in and out-of equilibrium characteristics of the CME.

The vector currents in in-out and in-in formalism may be cast in proper time as before,

$$\bar{j}^\mu := \langle \bar{\psi} \gamma^\mu \psi \rangle = i \lim_{y \rightarrow x} \text{tr} [\gamma^\mu S^c(x, y)] = -i \lim_{y \rightarrow x} \text{tr} [\gamma^\mu \not{D}_x \int_0^\infty ds g(x, y, s)], \quad (69)$$

$$j^\mu := \langle \langle \bar{\psi} \gamma^\mu \psi \rangle \rangle = i \lim_{y \rightarrow x} \text{tr} [\gamma^\mu S_{\text{in}}^c(x, y)] = -i \lim_{y \rightarrow x} \text{tr} [\gamma^\mu \not{D}_x \int_{\text{in}} ds g(x, y, s)]. \quad (70)$$

Using similar steps as outlined for Eq. (59), (where we found that the covariant derivative acting on the kernel in the  $x \rightarrow y$  limit vanished due to a translational invariance), one can find that the Euclidean equilibrium CME current,  $\bar{j}^3$  vanishes, as is understood in condensed matter applications.<sup>192</sup> Then as before, one can see the emergence of the CME in an out-of equilibrium context, here sourced through the Schwinger mechanism.

Calculations for the real-time CME follow closely to those done for the chiral density, Eq. (61), therefore let us simply outline some key steps. As before, we can eliminate terms without poles coming from the spin and boson path integral factors. The Dirac trace here is

$$\begin{aligned} \text{tr} \gamma^\mu \not{D} e^{-\frac{i}{2} e F \sigma s} &= 4 D_\nu \left\{ \cos(eBs) \cosh(eEs) g^{\mu\nu} \right. \\ &\quad \left. - \sin(eBs) \cosh(eEs) (-g^{\mu 1} g^{\nu 2} + g^{\mu 2} g^{\nu 1}) - \cos(eBs) \sinh(eEs) \epsilon^{\mu\nu 12} \right\}. \end{aligned} \quad (71)$$

Let us also note that  $z_0$  dependence vanishes in the  $x \rightarrow y$  limit since  $\partial^0 \theta(z_3^2 - z_0^2) = 0$ . We essentially find Eq. (61), however, with a sum over the Landau levels



corresponding to the  $\coth(\pi B/E)$  term included:

$$j^\mu = \frac{e^2 E B t}{2\pi^2} \coth\left(\frac{\pi B}{E}\right) \exp\left(-\frac{m^2 \pi}{e E}\right) \delta_3^\mu = 2\omega t \delta_3^\mu. \quad (72)$$

A current emerges in accordance with Schwinger’s formula given in Eq. (7) under the LLLA of the above. We find while the CME vanishes in Euclidean equilibrium, it reemerges out-of equilibrium in a real-time picture through the Schwinger mechanism in QED. The above expression and connection to the CME through the Schwinger mechanism was first examined in Ref. 13, relying on a Lorentz transformation of Schwinger’s formula. And that a current is generated from the Schwinger mechanism is indeed well known.<sup>176,194,196</sup> While all Landau levels have been kept in the above analysis, let us emphasize that the CME should only appear as a result of generated chirality. However we saw in Eqs. (53) and (54) that only the LLLA contributed to a net chirality.

We also noticed that these currents can also be computed through the equal-time Wigner function approaches.<sup>198–203</sup> Having seen the importance the Schwinger mechanism plays on both the anomaly and the CME, let us examine its effects on the chiral condensate.

## 8. Chiral Condensate

The chiral condensate possesses an interesting interplay with the chiral symmetry, and besides its finiteness giving rise to a baryon mass, the chiral condensate may be enhanced in an external magnetic field in what is known as magnetic catalysis.<sup>25–27,204</sup> Then it is an interesting extension, we explore here, to evaluate the chiral condensate in a strong electric field such that Schwinger pair production be producible. Also, to what effect does the out-of equilibrium process entail for dynamical mass; this too we can address here.

The chiral condensates both in and out-of equilibrium respectively are

$$\bar{\Sigma} := \langle \bar{\psi} \psi \rangle = i \lim_{y \rightarrow x} \text{tr} [S^c(x, y)], \quad (73)$$

$$\Sigma := \langle \langle \bar{\psi} \psi \rangle \rangle = i \lim_{y \rightarrow x} \text{tr} [S_{\text{in}}^c(x, y)]. \quad (74)$$

We first treat the magnetic catalysis case; this is simply the one with  $E = 0$ , and hence either of the expression above may be used. Let us also employ the LLLA as was used for the chiral density fluctuations. Then the chiral condensate can be found as

$$\begin{aligned} \bar{\Sigma}|_{E=0} &= -\frac{eB}{4\pi^2} m \int_0^\infty \frac{ds}{s} e^{-im^2 s} \cot(eBs) \\ &= -\frac{eB}{4\pi^2} m \int_{m^2/\Lambda^2}^\infty \frac{ds}{s} e^{-m^2 s} \coth(eBs) \\ &\simeq -\frac{eB}{4\pi^2} m \Gamma[0, m^2/\Lambda^2]. \end{aligned} \quad (75)$$

An ultraviolet cutoff has been introduced in the second step, where also a rotation in  $s \rightarrow -is$  has been done—making a connection to more familiar constructions.<sup>26,204</sup> Magnetic catalysis emerges for small  $m$  from an infinite negative curvature after solving the gap equation for the condensate stemming from the logarithmic singularity in the condensate,  $\Gamma[0, m^2/\Lambda^2] \simeq -\gamma_E + \ln(\Lambda^2/m^2)$ , where  $\gamma_E$  is the Euler-Mascheroni constant. Let us now examine how the condensate behaves under a parallel electric field starting with the Euclidean equilibrium case first.

The in-out chiral condensate can be found straightforwardly:

$$\begin{aligned}\bar{\Sigma} &= -\frac{e^2 EB}{4\pi^2} m \int_0^\infty ds e^{-im^2 s} \cot(eBs) \coth(eEs) \\ &= -\frac{e^2 EB}{4\pi^2} m \int_{m^2/\Lambda^2}^\infty ds e^{-m^2 s} \coth(eBs) \cot(eEs) \\ &\simeq -\frac{e^2 EB}{4\pi^2} m \int_{m^2/\Lambda^2}^\infty ds e^{-m^2 s} \cot(eEs) \\ &\simeq -\frac{eB}{4\pi^2} m \left[ \ln \frac{\Lambda^2 e^{-\gamma_E}}{2eE} - \text{Re}\psi\left(\frac{im^2}{2eE}\right) - \frac{i\pi}{e^{\pi m^2/(eE)} - 1} \right].\end{aligned}\quad (76)$$

In addition to the LLLA, we also approximate for large  $\Lambda$ ,  $e^{-m^2/\Lambda^2} \sim 1$  and also thereafter only leading order contributions of  $\Lambda^2$  have been kept.  $\psi(x)$  here is the digamma function. We can see in Eq. (76) that the logarithmic singularity with respect to  $m^2$  has disappeared.<sup>205</sup> Furthermore, there is a suppression of the condensate with the inclusion of the electric field; this we will explore in greater depth with the realization of Schwinger pair production provided by the in-in construction. Also in Eq. (76) we see there is an imaginary piece—as alluded to in Sec. 5.3. What is interesting is the form of the imaginary part resembles a bosonic-like distribution, with “temperature” in proper time given by  $\pi/(eE)$ . A similar distribution is also in fact present for the squared matrix element predicting the probability for a single particle pair to be found due to the Schwinger mechanism. That a “temperature” arises highlights a non-equilibrium nature, that we examine in the real-time picture below. Let us also mention that a temperature arises in the worldline picture from a dynamical gauge field in addition to the background gauge field through sphaleron transitions.<sup>206,207</sup> Furthermore, the real-time quantity is real as expected. Let us also point out that complex features have also been seen in QFTs under a finite  $\theta$ .<sup>208,209</sup> And, a topological  $\theta$  and our fields, Eq. (5) share similar quantum numbers, therefore complex observables would be anticipated. Last, let us also mention that one can recover Eq. (75) from Eq. (76) by noting the asymptotic expansion,  $\psi(x) \sim \ln x - 1/2x$  for large  $x$ .

We find for the in-in chiral condensate, Eq. (74),

$$\begin{aligned}\Sigma &= -\frac{e^2 EB}{4\pi^2} m \int_{in} ds e^{-im^2 s} \cot(eBs) \coth(eEs) \\ &= -\frac{e^2 EB}{4\pi^2} m \int_{1/\Lambda^2}^{\pi/eE-1/\Lambda^2} ds e^{-m^2 s} \coth(eBs) \cot(eEs)\end{aligned}$$

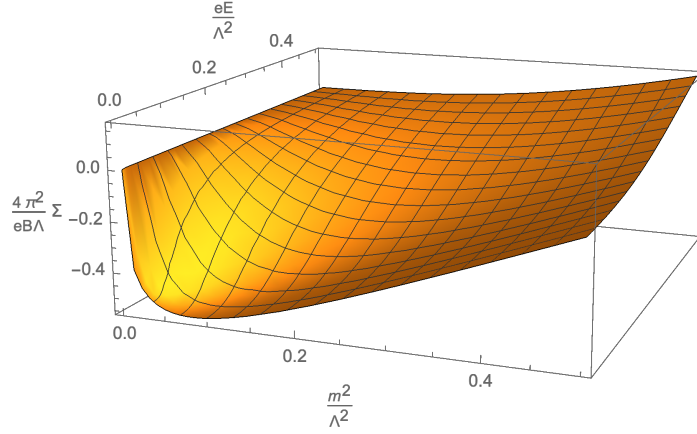


Fig. 9. In-in (out-of equilibrium) chiral condensate, Eq. (77) in parallel electric and magnetic fields. The dimensionless condensate is divided by  $eB/4\pi^2$  and the scale  $\Lambda$ . Condensate is depicted for background electric fields,  $eE/\Lambda^2$ , and mass,  $m^2/\Lambda^2$ . For large  $E$ , observe a melting of the condensate,  $\Sigma \rightarrow 0$ , and restoration of the chiral symmetry. The constituent mass is decreased from the Schwinger mechanism.

$$\simeq \left[ 1 - e^{-\pi m^2/(eE)} \right] \text{Re } \bar{\Sigma}, \quad (77)$$

under the LLLA.<sup>21</sup> As with the equilibrium case, Eq. (76), we see there are divergences; there are two poles here at  $s = 0, -i\pi/eE$ . However both UV divergences are approached the same way as for Eq. (76), therefore we regulate them similarly. The out-of equilibrium chiral condensate is depicted in Fig. 9. In contrast to magnetic catalysis, we see that with the addition of an electric field the chiral condensate is weakened,<sup>210–212</sup> which acts as an inverse magnetic catalysis effect. One may understand this process intuitively: While a magnetic field would act to strengthen the condensate through spin alignment, an electric field would act to pull the condensate apart, in effect weakening it.

A melting of the chiral condensate in an electric field might be observable in a condensed matter system. In contrast to QED, the energy gap in a Weyl semimetal is small, and it has been reasoned the Schwinger mechanism may be measured there.<sup>213</sup> Also, magnetic catalysis might be visible in Weyl semimetals,<sup>214</sup> and thus the semimetal may prove a vital means of accessing the melting behavior. One can also see Ref. 215, 216 for recent discussions in the electric field dependent chiral condensation.

## 9. Conclusions

Chirality generation from the QFT vacuum via the Schwinger mechanism has been examined. We have demonstrated the importance of vacuum states for the determination of expectation values. Notably, we showed that in-out expectation valued observables coincide with a scenario of Euclidean equilibrium, and in-in expectation

valued observables predict a situation out-of equilibrium. With an understanding of the difference of vacuum states for the production of chirality through Schwinger pair production, it was demonstrated how a heuristic picture of the process is indeed accurate. And also, with the understanding, it is reasoned the anomaly and related quantities should vanish in equilibrium.

It was found the pseudoscalar condensate, and hence axial Ward identity, by virtue of the Schwinger mechanism acquired mass dependence: A characteristic exponentially quadratic mass suppression was calculated out-of equilibrium, as too for a CME current. Also for the CME current as well as the chiral density current, a real-time (as would be expected from the in-in formalism) dependence emerged from a phase space factor. For the chiral density current, this was in accordance with the axial Ward identity. A chiral condensate with Schwinger mechanism effects was also discussed, where it was shown the condensate weakens, even vanishing, in a background electric field, in effect, acting as an inverse magnetic catalysis.

Here the beginnings of chirality generation by the Schwinger mechanism have been outlined, however future work is necessary to both expand and deepen our understanding. A notable shortcoming in the analysis presented here is the usage of homogeneous Abelian fields. While a general framework exists for handling in-out expectation values in a worldline picture, it is important to extend the worldline formalism for in-in expectation values to arbitrary fields. It would then be of interest to rigorously confirm the dependence of the Schwinger mechanism on the chiral anomaly in a non-Abelian background with topological winding number. And also for the cancellation of the anomaly in Euclidean equilibrium, it would be important to analyze similar non-trivial field types.

## Acknowledgments

The authors would like to thank Gaoqing Cao, Kenji Fukushima, Xu-Guang Huang, and Hidetoshi Taya for helpful discussions and comments.

## References

1. L. Barron, *Chem. Phys. Lett.* **123**, 423 (1986), doi:[https://doi.org/10.1016/0009-2614\(86\)80035-5](https://doi.org/10.1016/0009-2614(86)80035-5).
2. Y. Nambu and G. Jona-Lasinio, *Phys. Rev.* **122**, 345 (1961), doi:10.1103/PhysRev.122.345.
3. Y. Nambu and G. Jona-Lasinio, *Phys. Rev.* **124**, 246 (Oct 1961), doi:10.1103/PhysRev.124.246.
4. K. Fukushima, D. E. Kharzeev and H. J. Warringa, *Phys. Rev. D* **78**, 074033 (Oct 2008), doi:10.1103/PhysRevD.78.074033.
5. Z. Wang, Y. Sun, X.-Q. Chen, C. Franchini, G. Xu, H. Weng, X. Dai and Z. Fang, *Phys. Rev. B* **85**, 195320 (May 2012), doi:10.1103/PhysRevB.85.195320.
6. Z. Wang, H. Weng, Q. Wu, X. Dai and Z. Fang, *Phys. Rev. B* **88**, 125427 (Sep 2013), doi:10.1103/PhysRevB.88.125427.
7. M. Neupane, S.-Y. Xu, R. Sankar, N. Alidoust, G. Bian, C. Liu, I. Belopolski, T.-R.

- Chang, H.-T. Jeng, H. Lin, A. Bansil, F. Chou and M. Z. Hasan, *Nat. Commun.* **5**, 3786 (May 2014).
8. Z. K. Liu, J. Jiang, B. Zhou, Z. J. Wang, Y. Zhang, H. M. Weng, D. Prabhakaran, S.-K. Mo, H. Peng, P. Dudin, T. Kim, M. Hoesch, Z. Fang, X. Dai, Z. X. Shen, D. L. Feng, Z. Hussain and Y. L. Chen, *Nat. Mater.* **13**, 677 (May 2014).
  9. Q. Li, D. E. Kharzeev, C. Zhang, Y. Huang, I. Pletikosic, A. V. Fedorov, R. D. Zhong, J. A. Schneeloch, G. D. Gu and T. Valla, *Nature Phys.* **12**, 550 (2016), [arXiv:1412.6543 \[cond-mat.str-el\]](#), doi:10.1038/nphys3648.
  10. D. Kharzeev, K. Landsteiner, A. Schmitt and H.-U. Yee, *Strongly Interacting Matter in Magnetic Fields* (Springer Berlin Heidelberg, 2013).
  11. D. Kharzeev, A. Krasnitz and R. Venugopalan, *Phys. Lett. B* **545**, 298 (2002), doi:10.1016/S0370-2693(02)02630-8.
  12. T. Lappi and L. McLerran, *Nucl. Phys. A* **772**, 200 (2006), doi:10.1016/j.nuclphysa.2006.04.001.
  13. K. Fukushima, D. E. Kharzeev and H. J. Warringa, *Phys. Rev. Lett.* **104**, 212001 (2010), [arXiv:1002.2495 \[hep-ph\]](#), doi:10.1103/PhysRevLett.104.212001.
  14. A. Casher, H. Neuberger and S. Nussinov, *Phys. Rev. D* **20**, 179 (Jul 1979), doi:10.1103/PhysRevD.20.179.
  15. H. J. Warringa, *Phys. Rev. D* **86**, 085029 (2012), doi:10.1103/PhysRevD.86.085029.
  16. N. Tanji, *Annals Phys.* **325**, 2018 (2010), doi:10.1016/j.aop.2010.03.012.
  17. P. A. Morales Rodriguez, Dynamical Evolution of Quark Degrees of Freedom in the Relativistic Heavy Ion Collision within the Color Glass Condensate Framework, PhD thesis, Tokyo U. (2018).
  18. N. Tanji, *Phys. Rev. D* **98**, 014025 (2018), [arXiv:1805.00775 \[hep-ph\]](#), doi:10.1103/PhysRevD.98.014025.
  19. S. L. Adler, *Phys. Rev.* **177**, 2426 (Jan 1969), doi:10.1103/PhysRev.177.2426.
  20. J. S. Bell and R. Jackiw, *Nuovo Cim.* **A60**, 47 (1969), doi:10.1007/BF02823296.
  21. P. Copinger, K. Fukushima and S. Pu, *Phys. Rev. Lett.* **121**, 261602 (2018), [arXiv:1807.04416 \[hep-th\]](#), doi:10.1103/PhysRevLett.121.261602.
  22. V. Domcke, Y. Ema and K. Mukaida, *JHEP* **02**, 055 (2020), [arXiv:1910.01205 \[hep-ph\]](#), doi:10.1007/JHEP02(2020)055.
  23. D. E. Kharzeev, L. D. McLerran and H. J. Warringa, *Nucl. Phys.* **A803**, 227 (2008), [arXiv:0711.0950 \[hep-ph\]](#), doi:10.1016/j.nuclphysa.2008.02.298.
  24. A. Bzdak and V. Skokov, *Phys. Lett. B* **710**, 171 (2012), [arXiv:1111.1949 \[hep-ph\]](#), doi:10.1016/j.physletb.2012.02.065.
  25. K. G. Klimenko, *Theor. Math. Phys.* **90**, 1 (1992), doi:10.1007/BF01018812.
  26. V. P. Gusynin, V. A. Miransky and I. A. Shovkovy, *Phys. Rev. Lett.* **73**, 3499 (1994), doi:10.1103/PhysRevLett.73.3499, [Erratum: *Phys. Rev. Lett.* **76**, 1005(1996)].
  27. I. A. Shovkovy, *Lect. Notes Phys.* **871**, 13 (2013), doi:10.1007/978-3-642-37305-3\_2.
  28. J. S. Schwinger, *Phys. Rev.* **82**, 664 (1951), doi:10.1103/PhysRev.82.664, [,116(1951)].
  29. A. Belavin, A. Polyakov, A. Schwartz and Y. Tyupkin, *Phys. Lett. B* **59**, 85 (1975), doi:http://dx.doi.org/10.1016/0370-2693(75)90163-X.
  30. C. A. Baker *et al.*, *Phys. Rev. Lett.* **97**, 131801 (2006), doi:10.1103/PhysRevLett.97.131801.
  31. D. E. Kharzeev, *Annals Phys.* **325**, 205 (2010), doi:10.1016/j.aop.2009.11.002.
  32. X.-G. Huang, *Sci. Rep.* **6**, 20601 (2016), [arXiv:1506.03590 \[cond-mat.quant-gas\]](#), doi:10.1038/srep20601.
  33. D. Xiao, M.-C. Chang and Q. Niu, *Rev. Mod. Phys.* **82**, 1959 (Jul 2010), doi:10.1103/RevModPhys.82.1959.
  34. M.-C. Chang and Q. Niu, *J. of Phys.: Con. Matt.* **20**, 193202 (Apr 2008), doi:10.

- 1088/0953-8984/20/19/193202.
35. K. S. Novoselov, A. K. Geim, S. V. Morozov, D. Jiang, Y. Zhang, S. V. Dubonos, I. V. Grigorieva and A. A. Firsov, *Science* **306**, 666 (2004), doi:10.1126/science.1102896.
  36. S. Borisenko, Q. Gibson, D. Evtushinsky, V. Zabolotnyy, B. Büchner and R. J. Cava, *Phys. Rev. Lett.* **113**, 027603 (Jul 2014), doi:10.1103/PhysRevLett.113.027603.
  37. Z. K. Liu, B. Zhou, Y. Zhang, Z. J. Wang, H. M. Weng, D. Prabhakaran, S.-K. Mo, Z. X. Shen, Z. Fang, X. Dai, Z. Hussain and Y. L. Chen, *Science* **343**, 864 (2014), doi:10.1126/science.1245085.
  38. X. Huang, L. Zhao, Y. Long, P. Wang, D. Chen, Z. Yang, H. Liang, M. Xue, H. Weng, Z. Fang, X. Dai and G. Chen, *Phys. Rev. X* **5**, 031023 (Aug 2015), doi:10.1103/PhysRevX.5.031023.
  39. D. T. Son and B. Z. Spivak, *Phys. Rev. B* **88**, 104412 (2013), doi:10.1103/PhysRevB.88.104412.
  40. D. Kharzeev, J. Liao, S. Voloshin and G. Wang, *Prog. Part. Nucl. Phys.* **88**, 1 (2016), doi:https://doi.org/10.1016/j.ppnp.2016.01.001.
  41. STAR Collaboration Collaboration (B. I. Abelev *et al.*), *Phys. Rev. Lett.* **103**, 251601 (Dec 2009), doi:10.1103/PhysRevLett.103.251601.
  42. ALICE Collaboration Collaboration (B. Abelev *et al.*), *Phys. Rev. Lett.* **110**, 012301 (Jan 2013), doi:10.1103/PhysRevLett.110.012301.
  43. D. Kharzeev, *Phys. Lett. B* **633**, 260 (2006), [arXiv:hep-ph/0406125 \[hep-ph\]](#), doi:10.1016/j.physletb.2005.11.075.
  44. K. Fukushima, D. E. Kharzeev and H. J. Warringa, *Phys. Rev. D* **78**, 074033 (2008), [arXiv:0808.3382 \[hep-ph\]](#), doi:10.1103/PhysRevD.78.074033.
  45. D. E. Kharzeev and H.-U. Yee, *Phys. Rev. D* **83**, 085007 (2011), [arXiv:1012.6026 \[hep-th\]](#), doi:10.1103/PhysRevD.83.085007.
  46. Y. Burnier, D. E. Kharzeev, J. Liao and H.-U. Yee, *Phys. Rev. Lett.* **107**, 052303 (2011), [arXiv:1103.1307 \[hep-ph\]](#), doi:10.1103/PhysRevLett.107.052303.
  47. X.-G. Huang and J. Liao, *Phys. Rev. Lett.* **110**, 232302 (2013), [arXiv:1303.7192 \[nucl-th\]](#), doi:10.1103/PhysRevLett.110.232302.
  48. S. Pu, S.-Y. Wu and D.-L. Yang, *Phys. Rev. D* **89**, 085024 (2014), [arXiv:1401.6972 \[hep-th\]](#), doi:10.1103/PhysRevD.89.085024.
  49. Y. Jiang, X.-G. Huang and J. Liao, *Phys. Rev. D* **91**, 045001 (2015), [arXiv:1409.6395 \[nucl-th\]](#), doi:10.1103/PhysRevD.91.045001.
  50. S. Pu, S.-Y. Wu and D.-L. Yang, *Phys. Rev. D* **91**, 025011 (2015), [arXiv:1407.3168 \[hep-th\]](#), doi:10.1103/PhysRevD.91.025011.
  51. E. Gorbar, I. Shovkovy, S. Vilchinskii, I. Rudenok, A. Boyarsky and O. Ruchayskiy, *Phys. Rev. D* **93**, 105028 (2016), [arXiv:1603.03442 \[hep-th\]](#), doi:10.1103/PhysRevD.93.105028.
  52. E. Gorbar, V. Miransky, I. Shovkovy and P. Sukhachov, *Phys. Rev. B* **95**, 115202 (2017), [arXiv:1611.05470 \[cond-mat.mes-hall\]](#), doi:10.1103/PhysRevB.95.115202.
  53. J.-W. Chen, T. Ishii, S. Pu and N. Yamamoto, *Phys. Rev. D* **93**, 125023 (2016), [arXiv:1603.03620 \[hep-th\]](#), doi:10.1103/PhysRevD.93.125023.
  54. S. Ebihara, K. Fukushima and S. Pu, *Phys. Rev. D* **96**, 016016 (2017), [arXiv:1705.08611 \[hep-ph\]](#), doi:10.1103/PhysRevD.96.016016.
  55. Y. Hidaka and D.-L. Yang, *Phys. Rev. D* **98**, 016012 (2018), [arXiv:1801.08253 \[hep-th\]](#), doi:10.1103/PhysRevD.98.016012.
  56. Y. Bu, T. Demircik and M. Lublinsky, *JHEP* **05**, 071 (2019), [arXiv:1903.00896 \[hep-th\]](#), doi:10.1007/JHEP05(2019)071.
  57. Y. Bu, T. Demircik and M. Lublinsky, *JHEP* **01**, 078 (2019), [arXiv:1807.08467](#)

- [hep-th], doi:10.1007/JHEP01(2019)078.
58. Y. Bu, R.-G. Cai, Q. Yang and Y.-L. Zhang, *JHEP* **09**, 083 (2018), [arXiv:1803.08389 \[hep-th\]](#), doi:10.1007/JHEP09(2018)083.
  59. S. Y. Liu and Y. Yin (6 2020), [arXiv:2006.12421 \[nucl-th\]](#).
  60. M. A. Stephanov and Y. Yin, *Phys. Rev. Lett.* **109**, 162001 (2012), [arXiv:1207.0747 \[hep-th\]](#), doi:10.1103/PhysRevLett.109.162001.
  61. J.-W. Chen, J.-y. Pang, S. Pu and Q. Wang, *Phys. Rev. D* **89**, 094003 (2014), [arXiv:1312.2032 \[hep-th\]](#), doi:10.1103/PhysRevD.89.094003.
  62. J.-Y. Chen, D. T. Son, M. A. Stephanov, H.-U. Yee and Y. Yin, *Phys. Rev. Lett.* **113**, 182302 (2014), [arXiv:1404.5963 \[hep-th\]](#), doi:10.1103/PhysRevLett.113.182302.
  63. J.-Y. Chen, D. T. Son and M. A. Stephanov, *Phys. Rev. Lett.* **115**, 021601 (2015), [arXiv:1502.06966 \[hep-th\]](#), doi:10.1103/PhysRevLett.115.021601.
  64. D. T. Son and N. Yamamoto, *Phys. Rev.* **D87**, 085016 (2013), [arXiv:1210.8158 \[hep-th\]](#), doi:10.1103/PhysRevD.87.085016.
  65. C. Manuel and J. M. Torres-Rincon, *Phys. Rev.* **D89**, 096002 (2014), [arXiv:1312.1158 \[hep-ph\]](#), doi:10.1103/PhysRevD.89.096002.
  66. C. Manuel and J. M. Torres-Rincon, *Phys. Rev.* **D90**, 076007 (2014), [arXiv:1404.6409 \[hep-ph\]](#), doi:10.1103/PhysRevD.90.076007.
  67. S. Lin and A. Shukla, *JHEP* **06**, 060 (2019), [arXiv:1901.01528 \[hep-ph\]](#), doi:10.1007/JHEP06(2019)060.
  68. S. Lin and L. Yang, *Phys. Rev. D* **101**, 034006 (2020), [arXiv:1909.11514 \[nucl-th\]](#), doi:10.1103/PhysRevD.101.034006.
  69. J.-W. Chen, S. Pu, Q. Wang and X.-N. Wang, *Phys. Rev. Lett.* **110**, 262301 (2013), [arXiv:1210.8312 \[hep-th\]](#), doi:10.1103/PhysRevLett.110.262301.
  70. J.-W. Chen, J.-H. Gao, J. Liu, S. Pu and Q. Wang, *Phys. Rev. D* **88**, 074003 (2013), [arXiv:1305.1835 \[nucl-th\]](#), doi:10.1103/PhysRevD.88.074003.
  71. Y. Hidaka, S. Pu and D.-L. Yang, *Phys. Rev.* **D95**, 091901 (2017), [arXiv:1612.04630 \[hep-th\]](#), doi:10.1103/PhysRevD.95.091901.
  72. Y. Hidaka, S. Pu and D.-L. Yang, *Phys. Rev. D* **97**, 016004 (2018), [arXiv:1710.00278 \[hep-th\]](#), doi:10.1103/PhysRevD.97.016004.
  73. Y. Hidaka, S. Pu and D.-L. Yang, *Nucl. Phys. A* **982**, 547 (2019), [arXiv:1807.05018 \[nucl-th\]](#), doi:10.1016/j.nuclphysa.2018.10.033.
  74. A. Huang, S. Shi, Y. Jiang, J. Liao and P. Zhuang, *Phys. Rev.* **D98**, 036010 (2018), [arXiv:1801.03640 \[hep-th\]](#), doi:10.1103/PhysRevD.98.036010.
  75. J.-H. Gao, Z.-T. Liang, Q. Wang and X.-N. Wang, *Phys. Rev.* **D98**, 036019 (2018), [arXiv:1802.06216 \[hep-ph\]](#), doi:10.1103/PhysRevD.98.036019.
  76. Y.-C. Liu, L.-L. Gao, K. Mameda and X.-G. Huang, *Phys. Rev.* **D99**, 085014 (2019), [arXiv:1812.10127 \[hep-th\]](#), doi:10.1103/PhysRevD.99.085014.
  77. S.-Z. Yang, J.-H. Gao, Z.-T. Liang and Q. Wang (3 2020), [arXiv:2003.04517 \[hep-ph\]](#).
  78. N. Mueller and R. Venugopalan, *Phys. Rev.* **D97**, 051901 (2018), [arXiv:1701.03331 \[hep-ph\]](#), doi:10.1103/PhysRevD.97.051901.
  79. N. Mueller and R. Venugopalan, *Phys. Rev. D* **96**, 016023 (2017), [arXiv:1702.01233 \[hep-ph\]](#), doi:10.1103/PhysRevD.96.016023.
  80. Y. Sun, C. M. Ko and F. Li, *Phys. Rev.* **C94**, 045204 (2016), [arXiv:1606.05627 \[nucl-th\]](#), doi:10.1103/PhysRevC.94.045204.
  81. Y. Sun and C. M. Ko, *Phys. Rev.* **C95**, 034909 (2017), [arXiv:1612.02408 \[nucl-th\]](#), doi:10.1103/PhysRevC.95.034909.
  82. Y. Sun and C. M. Ko, *Phys. Rev.* **C96**, 024906 (Aug 2017), [arXiv:1706.09467 \[nucl-th\]](#), doi:10.1103/PhysRevC.96.024906.



83. Y. Sun and C. M. Ko, *Phys. Rev.* **C98**, 014911 (2018), [arXiv:1803.06043 \[nucl-th\]](#), doi:10.1103/PhysRevC.98.014911.
84. Y. Sun and C. M. Ko, *Phys. Rev.* **C99**, 011903 (2019), [arXiv:1810.10359 \[nucl-th\]](#), doi:10.1103/PhysRevC.99.011903.
85. W.-H. Zhou and J. Xu, *Phys. Rev.* **C98**, 044904 (2018), [arXiv:1810.01030 \[nucl-th\]](#), doi:10.1103/PhysRevC.98.044904.
86. W.-H. Zhou and J. Xu, *Phys. Lett.* **B798**, 134932 (2019), [arXiv:1904.01834 \[nucl-th\]](#), doi:10.1016/j.physletb.2019.134932.
87. S. Y. F. Liu, Y. Sun and C. M. Ko (2019), [arXiv:1910.06774 \[nucl-th\]](#).
88. J.-H. Gao and Z.-T. Liang, *Phys. Rev.* **D100**, 056021 (2019), [arXiv:1902.06510 \[hep-ph\]](#), doi:10.1103/PhysRevD.100.056021.
89. Z. Wang, X. Guo, S. Shi and P. Zhuang, *Phys. Rev.* **D100**, 014015 (2019), [arXiv:1903.03461 \[hep-ph\]](#), doi:10.1103/PhysRevD.100.014015.
90. N. Weickgenannt, X.-L. Sheng, E. Speranza, Q. Wang and D. H. Rischke, *Phys. Rev. D* **100**, 056018 (2019), [arXiv:1902.06513 \[hep-ph\]](#), doi:10.1103/PhysRevD.100.056018.
91. S. Li and H.-U. Yee, *Phys. Rev.* **D100**, 056022 (2019), [arXiv:1905.10463 \[hep-ph\]](#), doi:10.1103/PhysRevD.100.056022.
92. N. Weickgenannt, X.-L. Sheng, E. Speranza, Q. Wang and D. H. Rischke, Wigner function and kinetic theory for massive spin-1/2 particles, in *28th International Conference on Ultrarelativistic Nucleus-Nucleus Collisions (Quark Matter 2019) Wuhan, China, November 4-9, 2019*, (2020). [arXiv:2001.11862 \[hep-ph\]](#).
93. X.-L. Sheng, Q. Wang and X.-G. Huang (5 2020), [arXiv:2005.00204 \[hep-ph\]](#).
94. X. Guo (5 2020), [arXiv:2005.00228 \[hep-ph\]](#).
95. D.-L. Yang, K. Hattori and Y. Hidaka, *JHEP* **20**, 070 (2020), [arXiv:2002.02612 \[hep-ph\]](#), doi:10.1007/JHEP07(2020)070.
96. N. Weickgenannt, E. Speranza, X.-L. Sheng, Q. Wang and D. H. Rischke (5 2020), [arXiv:2005.01506 \[hep-ph\]](#).
97. S. Pu, V. Roy, L. Rezzolla and D. H. Rischke, *Phys. Rev.* **D93**, 074022 (2016), [arXiv:1602.04953 \[nucl-th\]](#), doi:10.1103/PhysRevD.93.074022.
98. V. Roy, S. Pu, L. Rezzolla and D. Rischke, *Phys. Lett.* **B750**, 45 (2015), [arXiv:1506.06620 \[nucl-th\]](#), doi:10.1016/j.physletb.2015.08.046.
99. S. Pu and D.-L. Yang, *Phys. Rev.* **D93**, 054042 (2016), [arXiv:1602.04954 \[nucl-th\]](#), doi:10.1103/PhysRevD.93.054042.
100. S. Pu and D.-L. Yang, *EPJ Web Conf.* **137**, 13021 (2017), [arXiv:1611.04840 \[hep-ph\]](#), doi:10.1051/epjconf/201713713021.
101. V. Roy, S. Pu, L. Rezzolla and D. H. Rischke, *DAE Symp. Nucl. Phys.* **62**, 926 (2017).
102. I. Siddique, R.-j. Wang, S. Pu and Q. Wang, *Phys. Rev.* **D99**, 114029 (2019), [arXiv:1904.01807 \[hep-ph\]](#), doi:10.1103/PhysRevD.99.114029.
103. R.-j. Wang, P. Copinger and S. Pu, Anomalous magnetohydrodynamics with constant anisotropic electric conductivities, in *28th International Conference on Ultrarelativistic Nucleus-Nucleus Collisions*, (4 2020). [arXiv:2004.06408 \[hep-ph\]](#).
104. G. Inghirami, L. Del Zanna, A. Beraudo, M. H. Moghaddam, F. Becattini and M. Bleicher, *Eur. Phys. J.* **C76**, 659 (2016), [arXiv:1609.03042 \[hep-ph\]](#), doi:10.1140/epjc/s10052-016-4516-8.
105. G. Inghirami, M. Mace, Y. Hirono, L. Del Zanna, D. E. Kharzeev and M. Bleicher (2019), [arXiv:1908.07605 \[hep-ph\]](#).
106. G. S. Denicol, X.-G. Huang, E. Molnar, G. M. Monteiro, H. Niemi, J. Noronha, D. H. Rischke and Q. Wang, *Phys. Rev.* **D98**, 076009 (2018), [arXiv:1804.05210 \[nucl-th\]](#), doi:10.1103/PhysRevD.98.076009.



107. G. S. Denicol, E. Molnar, H. Niemi and D. H. Rischke, *Phys. Rev.* **D99**, 056017 (2019), [arXiv:1902.01699 \[nucl-th\]](#), doi:10.1103/PhysRevD.99.056017.
108. Y. Jiang, S. Shi, Y. Yin and J. Liao, *Chin. Phys.* **C42**, 011001 (2018), [arXiv:1611.04586 \[nucl-th\]](#), doi:10.1088/1674-1137/42/1/011001.
109. S. Shi, Y. Jiang, E. Lilleskov and J. Liao, *Annals Phys.* **394**, 50 (2018), [arXiv:1711.02496 \[nucl-th\]](#), doi:10.1016/j.aop.2018.04.026.
110. S. Shi, Y. Jiang, E. Lilleskov and J. Liao, *PoS CPOD2017*, 021 (2018), [arXiv:1712.01386 \[nucl-th\]](#), doi:10.22323/1.311.0021.
111. B. Feng, D.-f. Hou, H. Liu, H.-c. Ren, P.-p. Wu and Y. Wu, *Phys. Rev. D* **95**, 114023 (2017), [arXiv:1702.07980 \[hep-ph\]](#), doi:10.1103/PhysRevD.95.114023.
112. Y. Wu, D. Hou and H.-c. Ren, *Phys. Rev. D* **96**, 096015 (2017), [arXiv:1601.06520 \[hep-ph\]](#), doi:10.1103/PhysRevD.96.096015.
113. S. Lin and L. Yang, *Phys. Rev. D* **98**, 114022 (2018), [arXiv:1810.02979 \[nucl-th\]](#), doi:10.1103/PhysRevD.98.114022.
114. M. Horvath, D. Hou, J. Liao and H.-c. Ren, *Phys. Rev. D* **101**, 076026 (2020), [arXiv:1911.00933 \[hep-ph\]](#), doi:10.1103/PhysRevD.101.076026.
115. B. Feng, D.-F. Hou and H.-C. Ren, *Phys. Rev. D* **99**, 036010 (2019), [arXiv:1810.05954 \[hep-ph\]](#), doi:10.1103/PhysRevD.99.036010.
116. D.-f. Hou and S. Lin, *Phys. Rev. D* **98**, 054014 (2018), [arXiv:1712.08429 \[hep-ph\]](#), doi:10.1103/PhysRevD.98.054014.
117. S. Lin, L. Yan and G.-R. Liang, *Phys. Rev. C* **98**, 014903 (2018), [arXiv:1802.04941 \[nucl-th\]](#), doi:10.1103/PhysRevC.98.014903.
118. C. Shi, X.-T. He, W.-B. Jia, Q.-W. Wang, S.-S. Xu and H.-S. Zong, *JHEP* **06**, 122 (2020), [arXiv:2004.09918 \[hep-ph\]](#), doi:10.1007/JHEP06(2020)122.
119. D. E. Kharzeev, J. Liao, S. A. Voloshin and G. Wang, *Prog. Part. Nucl. Phys.* **88**, 1 (2016), [arXiv:1511.04050 \[hep-ph\]](#), doi:10.1016/j.ppnp.2016.01.001.
120. J. Liao, *Pramana* **84**, 901 (2015), [arXiv:1401.2500 \[hep-ph\]](#), doi:10.1007/s12043-015-0984-x.
121. V. A. Miransky and I. A. Shovkovy, *Phys. Rept.* **576**, 1 (2015), [arXiv:1503.00732 \[hep-ph\]](#), doi:10.1016/j.physrep.2015.02.003.
122. X.-G. Huang, *Rept. Prog. Phys.* **79**, 076302 (2016), [arXiv:1509.04073 \[nucl-th\]](#), doi:10.1088/0034-4885/79/7/076302.
123. V. Koch, S. Schlichting, V. Skokov, P. Sorensen, J. Thomas, S. Voloshin, G. Wang and H.-U. Yee, *Chin. Phys. C* **41**, 072001 (2017), [arXiv:1608.00982 \[nucl-th\]](#), doi:10.1088/1674-1137/41/7/072001.
124. K. Fukushima, *Prog. Part. Nucl. Phys.* **107**, 167 (2019), [arXiv:1812.08886 \[hep-ph\]](#), doi:10.1016/j.ppnp.2019.04.001.
125. A. Bzdak, S. Esumi, V. Koch, J. Liao, M. Stephanov and N. Xu (2019), [arXiv:1906.00936 \[nucl-th\]](#).
126. J. Zhao and F. Wang, *Prog. Part. Nucl. Phys.* **107**, 200 (2019), [arXiv:1906.11413 \[nucl-ex\]](#), doi:10.1016/j.ppnp.2019.05.001.
127. F.-Q. Wang and J. Zhao, *Nucl. Sci. Tech.* **29**, 179 (2018), doi:10.1007/s41365-018-0520-z.
128. Y.-C. Liu and X.-G. Huang, *Nucl. Sci. Tech.* **31**, 56 (2020), [arXiv:2003.12482 \[nucl-th\]](#), doi:10.1007/s41365-020-00764-z.
129. J.-H. Gao, G.-L. Ma, S. Pu and Q. Wang (5 2020), [arXiv:2005.10432 \[hep-ph\]](#).
130. F. Sauter, *Zeitschrift für Physik* **69**, 742 (Nov 1931), doi:10.1007/BF01339461.
131. W. Heisenberg and H. Euler, *Z. Phys.* **98**, 714 (1936), doi:10.1007/BF01343663.
132. O. Klein, *Z. Phys.* **53**, 157 (1929), doi:10.1007/BF01339716.
133. S. W. Hawking, *Commun. Math. Phys.* **43**, 199 (Aug 1975), doi:10.1007/BF02345020.

- 134. W. G. Unruh, *Phys. Rev. D* **14**, 870 (Aug 1976), doi:10.1103/PhysRevD.14.870.
- 135. P. W. Higgs, *Phys. Rev. Lett.* **13**, 508 (1964), doi:10.1103/PhysRevLett.13.508.
- 136. G. V. Dunne, *Int. J. Mod. Phys. A* **25**, 2373 (2010), doi:10.1142/9789814289931\_0060, 10.1142/S0217751X10049657.
- 137. A. Yildiz and P. H. Cox, *Phys. Rev. D* **21**, 1095 (1980), doi:10.1103/PhysRevD.21.1095.
- 138. J. Ambjorn and R. J. Hughes, *Annals Phys.* **145**, 340 (1983), doi:http://dx.doi.org/10.1016/0003-4916(83)90187-2.
- 139. M. Gyulassy and A. Iwazaki, *Phys. Lett. B* **165**, 157 (1985), doi:https://doi.org/10.1016/0370-2693(85)90711-7.
- 140. R. Schutzhold, H. Gies and G. Dunne, *Phys. Rev. Lett.* **101**, 130404 (2008), doi:10.1103/PhysRevLett.101.130404.
- 141. L. Keldysh, *Sov. Phys. JETP* **20**, 1307 (Nov 1965).
- 142. G. V. Dunne, H. Gies and R. Schutzhold, *Phys. Rev. D* **80**, 111301 (Dec 2009), doi:10.1103/PhysRevD.80.111301.
- 143. A. Monin and M. B. Voloshin, *Phys. Rev. D* **81**, 025001 (Jan 2010), doi:10.1103/PhysRevD.81.025001.
- 144. A. Monin and M. B. Voloshin, *Phys. Rev. D* **81**, 085014 (Apr 2010), doi:10.1103/PhysRevD.81.085014.
- 145. H. Taya, *Phys. Rev. D* **99**, 056006 (Mar 2019), doi:10.1103/PhysRevD.99.056006.
- 146. X.-G. Huang and H. Taya, *Phys. Rev. D* **100**, 016013 (Jul 2019), doi:10.1103/PhysRevD.100.016013.
- 147. H. Taya, *Phys. Rev. Research* **2**, 023257 (Jun 2020), doi:10.1103/PhysRevResearch.2.023257.
- 148. G. Torgrimsson, C. Schneider, J. Oertel and R. Schutzhold, *JHEP* **06**, 043 (2017), [arXiv:1703.09203 \[hep-th\]](https://arxiv.org/abs/1703.09203), doi:10.1007/JHEP06(2017)043.
- 149. G. Torgrimsson, *Phys. Rev. D* **99**, 096002 (May 2019), doi:10.1103/PhysRevD.99.096002.
- 150. X.-G. Huang, M. Matsuo and H. Taya, *Progress of Theoretical and Experimental Physics* **2019** (11 2019), doi:10.1093/ptep/ptz112, 113B02.
- 151. C. Kohlfurst, M. Mitter, G. von Winckel, F. Hebenstreit and R. Alkofer, *Phys. Rev. D* **88**, 045028 (2013), doi:10.1103/PhysRevD.88.045028.
- 152. M. Orthaber, F. Hebenstreit and R. Alkofer, *Phys. Lett. B* **698**, 80 (2011), doi:10.1016/j.physletb.2011.02.053.
- 153. S. Vajna, B. Dóra and R. Moessner, *Phys. Rev. B* **92**, 085122 (Aug 2015), doi:10.1103/PhysRevB.92.085122.
- 154. M. F. Linder, A. Lorke and R. Schützhold, *Phys. Rev. B* **97**, 035203 (Jan 2018), doi:10.1103/PhysRevB.97.035203.
- 155. D. Allor, T. D. Cohen and D. A. McGady, *Phys. Rev. D* **78**, 096009 (Nov 2008), doi:10.1103/PhysRevD.78.096009.
- 156. B. Dóra and R. Moessner, *Phys. Rev. B* **81**, 165431 (Apr 2010), doi:10.1103/PhysRevB.81.165431.
- 157. L. D. Landau, *Phys. Z. Sowjet.* **2**, 46 (1932).
- 158. C. Zener and R. H. Fowler, *Proc. R. Soc. (London) A* **137**, 696 (1932), doi:10.1098/rspa.1932.0165.
- 159. J. Kim, S. S. Baik, S. H. Ryu, Y. Sohn, S. Park, B.-G. Park, J. Denlinger, Y. Yi, H. J. Choi and K. S. Kim, *Science* **349**, 723 (2015), doi:10.1126/science.aaa6486.
- 160. E. Kane, *J. Phys. Chem. Solids* **12**, 181 (1960), doi:https://doi.org/10.1016/0022-3697(60)90035-4.
- 161. C. Bamber, S. J. Boege, T. Koffas, T. Kotseroglou, A. C. Melissinos, D. D. Meyer-

- hofer, D. A. Reis, W. Ragg, C. Bula, K. T. McDonald, E. J. Prebys, D. L. Burke, R. C. Field, G. Horton-Smith, J. E. Spencer, D. Walz, S. C. Berridge, W. M. Bugg, K. Shmakov and A. W. Weidemann, *Phys. Rev. D* **60**, 092004 (Oct 1999), doi:10.1103/PhysRevD.60.092004.
162. M. Marklund and J. Lundin, *Eur. Phys. J.* **D55**, 319 (2009), doi:10.1140/epjd/e2009-00169-6.
163. G. V. Dunne, *Eur. Phys. J.* **D55**, 327 (2009), doi:10.1140/epjd/e2009-00022-0.
164. A. Ringwald, Boiling the Vacuum with An X-Ray Free Electron Laser, in *Quantum Aspects of Beam Physics 2003*, (Oct 2004), pp. 149–163.
165. T. Heinzl and A. Ilderton, *Eur. Phys. J.* **D55**, 359 (2009), doi:10.1140/epjd/e2009-00113-x.
166. A. Gonoskov, S. Bastrakov, E. Efimenko, A. Ilderton, M. Marklund, I. Meyerov, A. Muraviev, A. Sergeev, I. Surmin and E. Wallin, *Phys. Rev. E* **92**, 023305 (Aug 2015), doi:10.1103/PhysRevE.92.023305.
167. J. Bloczynski, X.-G. Huang, X. Zhang and J. Liao, *Phys. Lett.* **B718**, 1529 (2013), [arXiv:1209.6594 \[nucl-th\]](#), doi:10.1016/j.physletb.2012.12.030.
168. W.-T. Deng and X.-G. Huang, *Phys. Rev.* **C85**, 044907 (2012), [arXiv:1201.5108 \[nucl-th\]](#), doi:10.1103/PhysRevC.85.044907.
169. V. Roy and S. Pu, *Phys. Rev.* **C92**, 064902 (2015), [arXiv:1508.03761 \[nucl-th\]](#), doi:10.1103/PhysRevC.92.064902.
170. H. Li, X.-l. Sheng and Q. Wang, *Phys. Rev.* **C94**, 044903 (2016), [arXiv:1602.02223 \[nucl-th\]](#), doi:10.1103/PhysRevC.94.044903.
171. STAR Collaboration (J. Adam *et al.*) (10 2019), [arXiv:1910.12400 \[nucl-ex\]](#).
172. S. Klein, A. Mueller, B.-W. Xiao and F. Yuan, *Phys. Rev. Lett.* **122**, 132301 (2019), [arXiv:1811.05519 \[hep-ph\]](#), doi:10.1103/PhysRevLett.122.132301.
173. C. Li, J. Zhou and Y.-J. Zhou, *Phys. Lett. B* **795**, 576 (2019), [arXiv:1903.10084 \[hep-ph\]](#), doi:10.1016/j.physletb.2019.07.005.
174. W. Zha, J. D. Brandenburg, Z. Tang and Z. Xu, *Phys. Lett. B* **800**, 135089 (2020), [arXiv:1812.02820 \[nucl-th\]](#), doi:10.1016/j.physletb.2019.135089.
175. W. Zha, L. Ruan, Z. Tang, Z. Xu and S. Yang, *Phys. Lett. B* **781**, 182 (2018), [arXiv:1804.01813 \[hep-ph\]](#), doi:10.1016/j.physletb.2018.04.006.
176. E. Fradkin, D. Guitman and S. Shvartsman, *Quantum electrodynamics: with unstable vacuum* (Springer-Verlag, 1991).
177. T. D. Cohen and D. A. McGady, *Phys. Rev. D* **78**, 036008 (2008), doi:10.1103/PhysRevD.78.036008.
178. G. V. Dunne, Heisenberg-Euler effective Lagrangians: Basics and extensions, in *From fields to strings: Circumnavigating theoretical physics*, 2004 pp. 445–522.
179. J. Ambjorn, J. Greensite and C. Peterson, *Nuclear Physics B* **221**, 381 (1983), doi:https://doi.org/10.1016/0550-3213(83)90585-0.
180. P. I. Fomin, V. A. Miransky and Yu. A. Sitenko, *Phys. Lett. B* **64**, 444 (1976), doi:10.1016/0370-2693(76)90117-9.
181. C. Schubert, *Phys. Rept.* **355**, 73 (2001), doi:10.1016/S0370-1573(01)00013-8.
182. O. Corradini and C. Schubert, Spinning Particles in Quantum Mechanics and Quantum Field Theory (2015). [arXiv:1512.08694 \[hep-th\]](#).
183. M. D. Schwartz, *Quantum Field Theory and the Standard Model* (Cambridge University Press, 2014).
184. R. P. Feynman, *Phys. Rev.* **80**, 440 (1950), doi:10.1103/PhysRev.80.440.
185. R. P. Feynman, *Phys. Rev.* **84**, 108 (1951), doi:10.1103/PhysRev.84.108.
186. K. Hattori, K. Itakura and S. Ozaki (1 2020), [arXiv:2001.06131 \[hep-ph\]](#).
187. J. S. Schwinger, *J. Math. Phys.* **2**, 407 (1961), doi:10.1063/1.1703727.

188. G. Baym and L. P. Kadanoff, *Phys. Rev.* **124**, 287 (1961), doi:10.1103/PhysRev.124.287.
189. R. D. Jordan, *Phys. Rev. D* **33**, 444 (Jan 1986), doi:10.1103/PhysRevD.33.444.
190. G. V. Dunne and C. Schubert, *Phys. Rev. D* **72**, 105004 (2005), doi:10.1103/PhysRevD.72.105004.
191. I. K. Affleck, O. Alvarez and N. S. Manton, *Nucl. Phys. B* **197**, 509 (1982), doi:10.1016/0550-3213(82)90455-2.
192. N. Yamamoto, *Phys. Rev. D* **92**, 085011 (2015), doi:10.1103/PhysRevD.92.085011.
193. K. Fujikawa, *Phys. Rev. Lett.* **42**, 1195 (1979), doi:10.1103/PhysRevLett.42.1195.
194. S. P. Gavrilov and D. M. Gitman, *Phys. Rev. D* **78**, 045017 (Aug 2008), doi:10.1103/PhysRevD.78.045017.
195. A. I. Nikishov, *Zh. Eksp. Teor. Fiz.* **57**, 1210 (1969).
196. N. Tanji, *Annals of Physics* **324**, 1691 (2009), doi:https://doi.org/10.1016/j.aop.2009.03.012.
197. A. I. Nikishov, *Journal of Soviet Laser Research* **6(6)**, 619 (11 1985), doi:https://doi.org/10.1007/BF01120143.
198. P.-f. Zhuang and U. W. Heinz, *Phys. Rev. D* **53**, 2096 (1996), [arXiv:hep-ph/9510206](#), doi:10.1103/PhysRevD.53.2096.
199. P.-f. Zhuang and U. W. Heinz, *Phys. Rev. D* **57**, 6525 (1998), [arXiv:hep-ph/9610438](#), doi:10.1103/PhysRevD.57.6525.
200. F. Hebenstreit, R. Alkofer and H. Gies, *Phys. Rev. D* **82**, 105026 (2010), [arXiv:1007.1099 \[hep-ph\]](#), doi:10.1103/PhysRevD.82.105026.
201. S. Mao and D. H. Rischke, *Phys. Lett. B* **792**, 149 (2019), [arXiv:1812.06684 \[hep-th\]](#), doi:10.1016/j.physletb.2019.03.034.
202. X.-L. Sheng, R.-H. Fang, Q. Wang and D. H. Rischke, *Phys. Rev.* **D99**, 056004 (2019), [arXiv:1812.01146 \[hep-ph\]](#), doi:10.1103/PhysRevD.99.056004.
203. X.-L. Sheng, Wigner Function for Spin-1/2 Fermions in Electromagnetic Fields, PhD thesis, Frankfurt U. (2019).
204. V. P. Gusynin, V. A. Miransky and I. A. Shovkovy, *Phys. Lett. B* **349**, 477 (1995), doi:10.1016/0370-2693(95)00232-A.
205. L. Wang, G. Cao, X.-G. Huang and P. Zhuang, *Phys. Lett. B* **780**, 273 (2018), doi:10.1016/j.physletb.2018.03.018.
206. O. Gould and A. Rajantie, *Phys. Rev. D* **96**, 076002 (Oct 2017), doi:10.1103/PhysRevD.96.076002.
207. O. Gould, A. Rajantie and C. Xie, *Phys. Rev. D* **98**, 056022 (Sep 2018), doi:10.1103/PhysRevD.98.056022.
208. D. Boer and J. K. Boomsma, *Phys. Rev. D* **78**, 054027 (2008), doi:10.1103/PhysRevD.78.054027.
209. K. Mameda, *Nucl. Phys. B* **889**, 712 (2014), doi:10.1016/j.nuclphysb.2014.11.002.
210. H. Suganuma and T. Tatsumi, *Annals of Physics* **208**, 470 (1991), doi:https://doi.org/10.1016/0003-4916(91)90304-Q.
211. H. Suganuma and T. Tatsumi, *Progress of Theoretical Physics* **90**, 379 (08 1993), doi:10.1143/ptp/90.2.379.
212. G. Cao, *Physics Letters B* **806**, 135477 (2020), doi:https://doi.org/10.1016/j.physletb.2020.135477.
213. S. Vajna, B. Dora and R. Moessner, *Phys. Rev. B* **92**, 085122 (2015), doi:10.1103/PhysRevB.92.085122.
214. B. Roy and J. D. Sau, *Phys. Rev. B* **92**, 125141 (Sep 2015), doi:10.1103/PhysRevB.92.125141.
215. G. Cao, *Physics Letters B* **806**, 135477 (Jul 2020), doi:10.1016/j.physletb.2020.

135477.

216. G. Cao, *Physical Review D* **101** (May 2020), doi:10.1103/physrevd.101.094027.